Design and analysis of laser-cut based moment resisting passing-through I-beam-to-CHS column joints

R. Das, C.A. Castiglioni, Maël Couchaux, B. Hoffmeister, H. Degee

Design and Analysis of Laser-Cut based Moment Resisting passing-through I-Beam-to-CHS Column Joints

Rajarshi Das[a,1], Carlo A. Castiglioni[b], Mael Couchaux[c], Benno Hoffmeister[d], Herve Degee[a]

[a] Construction Engineering Research Group, Hasselt University, Hasselt, Belgium
[b] Department of Architecture, Built Environment and Construction Engineering, Politecnico di Milano, Italy; Technical Director, Fincon Consulting Italia srl, Italy
[c] Department of Civil and Urban Engineering, National Institute of Applied Sciences of Rennes, France
[d] Institute of Steel Construction, RWTH Aachen University, Germany

Abstract

Conventional circular hollow section (CHS) connections are often prone to severe local distortion of the CHS column surface, premature flange fractures and demand excessive welding quantity due to much-needed local stiffeners, gusset plates or the direct welding technique. This results in an unavoidable complexity, which leads to a possible economic disadvantage. This paper proposes an innovative I-beam-to-CHS-column "passing-through" connection, which avoids the foretold drawbacks and increases the structural performance of these joints. The moment-resisting connection studied in this article was developed during the research project LASTEICON. It consists of primary beams connected to an I-beam passing through the CHS column through slots obtained via Laser Cutting Technology. The characterization of the ultimate resistance of the proposed connection under symmetrical and antisymmetrical loading conditions in bending is studied in detail. This is performed through a parametric study based on finite element (FE) models, which are primarily validated through an experimental campaign. Encouraging agreements obtained between the numerical and experimental results in terms of joint stiffness as well as joint resistance are presented. Moreover, different failure modes are identified and further characterized by

[1] corresponding author, e-mail address: rajarshi.das@uhasselt.be

developing comprehensive guidelines to design the proposed connection. Analytical calculations for several case studies are performed following the proposed design procedure and the results are compared with numerical as well as experimental results. Promising agreement is achieved, therefore confirming its practical implementation. Ultimately, the "passing-through" connections are compared with conventional (direct weld) joints to highlight the former's advantages from a structural perspective.

Keywords: Beam-to-CHS-column connection; Tubular structures; CHS joints; Hollow section joints; Through Beam connections; Passing-through joints.

List of symbols

A_{vb}	Through I-beam shear area
b	Through I-beam flange width
C_f	Compressive force in the through I-beam flange
d_b	Through I-beam depth
d_c	CHS column diameter
f_b	Punching shear stress
f_y	Material yield stress of steel
f_{yb}	Material yield stress of the through I-beam
f_{yc}	Material yield stress of the CHS column
f_{yw}	Material yield stress of the through I-beam web
L_b	Overall span of the beam
L_c	CHS column length
LC1	Load Case 1: Monotonic gravitation/symmetric loading
LC2	Load Case 2: Monotonic opposite bending loading
M_{bp}	Bending moment corresponding to the punching shear stress
$M_{b,opp}$	Moments developed at either face of the CHS under LC2
$M_{b,sym}$	Moments developed at either face of the CHS under LC1
$M_{b,Rd,opp}$	Flexural resistance of the joint under LC2
$M_{b,Rd,sym}$	Flexural resistance of the joint under LC1
$M_{ip,1,Rd}$	In-plane moment resistance of the CHS
$M_{pl,Rd,beam}$	Flexural resistance of the through I-beam
$M_{Rd,CHS}$	Flexural resistance of the CHS
$N_{1,Rd}$	Transverse tensile/compressive resistance of the CHS chord face
P	Vertical load at the free end of the main I-beam
t_c	CHS column thickness

t_f	Through I-beam flange thickness
t_w	Through I-beam web thickness
T_f	Tensile force in the through I-beam flange
V_{bb}	Shear corresponding to $M_{pl,Rd,beam}$
V_{bc}	Shear corresponding to $M_{pl,Rd,CHS}$
V_{bj}	Shear corresponding to $M_{b,Rd,opp}$
V_{bp}	Shear corresponding to M_{bp}
$V_{bu,opp}$	Joint ultimate strength under LC2
V_c	Shear in the CHS column
V_{joint}	Shear strength of the joint
V_n	Total joint resistance
$V_{pl,Rd,beam}$	Shear resistance of the through I-beam
V_u	Effective horizontal shear in the joint panel
V_{wn}	Shear strength of the I-beam web
$W_{eff,CHS}$	Effective section modulus of the CHS
$W_{el,CHS}$	Elastic section modulus of the CHS
$W_{el,beam}$	Elastic section modulus of the through I-beam
W_{pl}	Plastic section modulus of the through I-beam

1. INTRODUCTION

A current area of interest in structural engineering is the search for ways to improve the connections between hollow and open sections by limiting the complexity inherent to this joint type. Over the last few decades, engineers worldwide have strived to introduce new concepts to these joints in order to exploit the outstanding structural and architectural properties of Hollow Section (HS) profiles. These beneficial properties range from excellent resistance in terms of compression, tension as well as bending in all directions [1], their simple application in lightweight structures, the reduced need for fire protection measures in comparison with equivalent H-section and the possible establishment of composite behaviour by simply filling the HS columns with concrete. The Committee for International Development and Education on Construction of Tubular structures (CIDECT) has provided the necessary design guides [2-5] to design different types of open-to-hollow section joint connections. Some examples of these are shown in Fig. 1. A number of research studies [6-8]

have further extended similar design concepts through a component-based approach, which has already provided a clearer understanding regarding their structural behaviour.

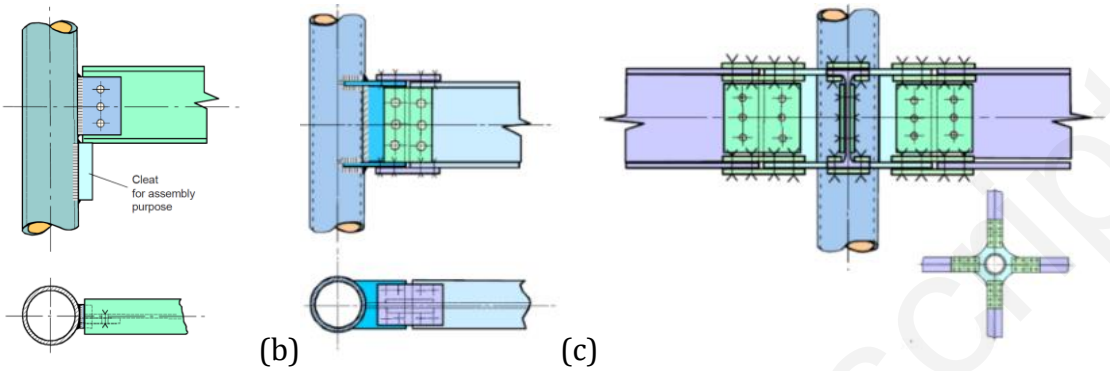

Fig. 1. *Examples of (a) one-way nominally pinned, (b) one-way moment resisting and (c) four-way moment resisting joints between open section and CHS investigated by CIDECT* [1]

Among several types of steel connections, the I-beam-to-CHS column connection has often proved to be complicated. In today's industry, I-beam-to-CHS connections are generally constructed by connecting I-beams to the CHS columns either by direct welding or by adopting local stiffeners and gusset plates. The first solution, i.e. the direct welding technique, causes a vulnerability towards severe local distortion on the CHS column and premature flange fractures. This was observed in a number of components- and full-scale tests done in a European Coal and Steel Community (ECSC) research program [9]. Schneider and Alostaz [10] also highlighted the similar issue by testing several directly welded and unstiffened beam-to-CHS connection prototypes. In order to get rid of such high amount of concentrated local stresses on the CHS and improve the connections, researches [11-12] adopted the second solution i.e. using local stiffeners and gusset plates. Wang et al. [11] used outer ring diaphragms to stiffen the I-beam-to-CHS connections with weak beams or weak columns. The weak beam joints (i.e. beam resistance - lower than the CHS connection) unexceptionally

exhibited final fracture at the link between the diaphragm and the beam flange while the weak column joints (i.e. CHS connection resistance - lower than the beam) demonstrated better seismic performance and ductility. Sabbagh et al. [12] investigated similar full strength I-beam-to-CHS moment-resisting joints for earthquake applications with external diaphragm plates bolted to the beam and welded to the circumference of the column. The partial contributions of the web panel and other connection components were highlighted in this study. The authors recommended avoiding excessive yielding and distortion of the web panel, as well as large stress concentration in the diaphragms since these can lead to weld fracture between the diaphragm plates and the column. However, as indicated by several researches in Japan [13-16], adoption of local stiffeners leads to an excessive welding quantity, which can cause both economic and practical difficulties during the joint fabrication and damages the aesthetics of the design. The cost of steel fabrication can account for 30-40% of the global project budget [17], with joint assemblage consuming the major share. Using local stiffeners or plates increases the joint complexity of the connection and can therefore increase this cost to an even higher extent. For this reason, their use in structural construction has not yet been prevalent even though several design guides and research studies had been published regarding the I-beam-to-CHS column connections.

In order to improve the I-beam-to-CHS column connections, a few types of connections were studied at a very preliminary stage with a “passing-through” approach in which steel elements were inserted or embedded through another element consisting of pure steel or concrete infilled composite hollow section column [18-21]. In 2010, Mirghaderi et al. [18] depicted the force transfer mechanism of connections constructed by a vertical plate passing through a Rectangular Hollow Section (RHS) column. In addition, these vertical

plates were welded to the column flanges and the main beams were connected to the through plate. The authors suggested a design approach to determine the dimensions of the through plate and other pertinent parts. Voth and Packer [19-20] conducted a comparison study between T-type conventional (Branch) and "passing-through" plate-to-CHS connections with experimental as well as numerical investigations and pointed out the advantages offered by the "passing-through" mechanism. Although, several studies provide substantial knowledge regarding the "passing-through" approach, most of them use plates as the "through" member. Therefore, a clear understanding cannot be gathered regarding a "through" I-beam section, which provides the necessary motivation behind this research study. An exception to this is found in the work of Alostaz and Schneider [21], which used a girder section as the "through" member inside a concrete filled CHS column. The moment-rotation behavior of this configuration was further compared with five different I-beam-to-CHS column connection types. The authors concluded that continuing the girder through the CHS column provides the most favorable inelastic connection behavior as it minimizes the local distortions occurring in the CHS column wall. However, a connection with a concrete filled composite HS column produces significant differences in the force-transfer mechanism compared to a pure steel HS column. This limits the available knowledge for the "passing-through" steel connections between an open and a hollow section. More details about the available literature was previously documented as a first study [22].

A novel moment resisting joint configuration is investigated in this research and is designated further as the "LASTEICON" connection (Fig. 2). This connection was initially proposed through a project [23] funded by the European Commission, where an I-beam passes through the CHS column via laser cut slots made on the column surface and the

primary beams ("*main*" I-beams) are connected to both ends of the passing through member ("*through*" member). The through member ("*Through I-beam*" in Fig. 2a) is welded to the outer face of the CHS column and connected to the "main" I beams by welded plate/beam splice connections. The applied moment is effectively transferred by the through member to the CHS column, whereas, the CHS column contributes significantly to the overall resistance of the connection against the transverse tensile/compressive forces. Although previous studies used such a "passing-through" concept, detailed results reflecting this behavior were not achieved due to practical difficulties regarding the traditional cutting process, fabrication of the connection as well as controlling the tolerance issues. However, thanks to the Laser Cutting Technology (LCT), advantages such as, significant reduction in welding quantities, swift fabrication process, controlled management of tolerance, better precision and minimization of human error through computer-programmed automation, facilitated this investigation in performing an in-depth understanding of the "passing-through" I-beam-to-CHS column connection. Further details regarding the complete fabrication process using LCT as well as a cost estimation was discussed in a previous article [24] in which the proposed LASTEICON connection is compared with the conventional connection from an economic perspective. A detailed description of the laser cutting procedure was also provided to show its potential in the steel construction sector.

This present study investigates the proposed LASTEICON I-beam-to-CHS column connection using a comprehensive parametric study. Results obtained from detailed analytical calculations are further validated by FE numerical simulations and preliminary experimental endorsements. The primary objective is to identify and characterize the

behavioral influences caused by each parameter and propose a constructive design approach for the future designers.

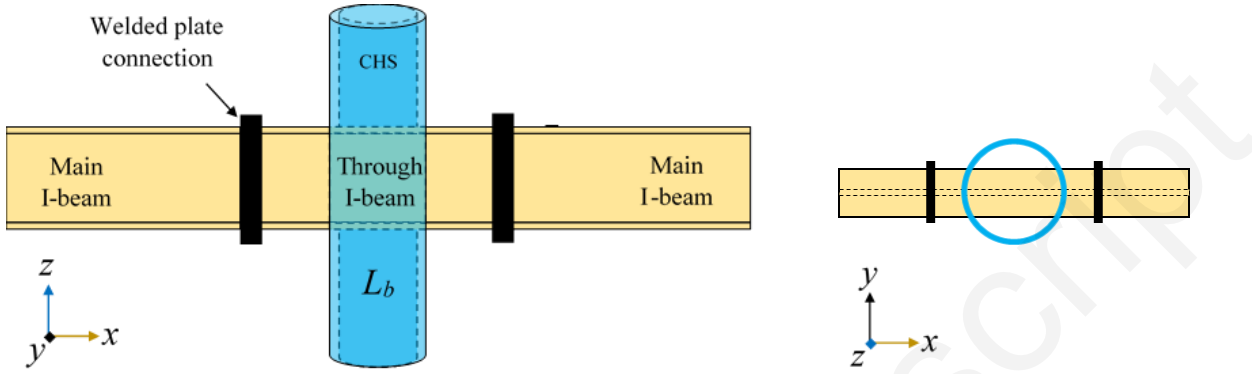

Fig. 2. *Schematic diagrams of the proposed LASTEICON connection*

2. DESIGN APPROACH FOR THE LASTEICON TWO-WAY MOMENT RESISTING JOINTS WITH I-PROFILE PASSING THROUGH A CHS COLUMN

A new design approach was developed for the proposed I-beam-to-CHS column connection based on detailed FE parametric studies, preliminary experimental validations and conceptual understandings obtained from the available literature [8, 18, and 25]. Relevant geometric notations necessary for the design procedure are shown in Fig. 3. Two different load cases were considered to gather a detailed understanding of the moment connection behaviour. Load Case 1 (LC1) defines a monotonic loading case with two unidirectional vertical loads, each acting at the end points of the main beam as shown in Fig. 4a, whereas Load Case 2 (LC2) designates a monotonic opposite bending load case, where both the loads are applied in an opposite direction, as shown in Fig. 4b. Design procedures were developed for each loading scenario. This study primarily focuses on deriving the joint strength of the "passing-through" zone. Hence, the connections between the "through" member and "main"

I-beams were assumed adequately strong in all cases. These connections can however be designed according to well-known classical approaches (according to Eurocodes) and are therefore not discussed in this study.

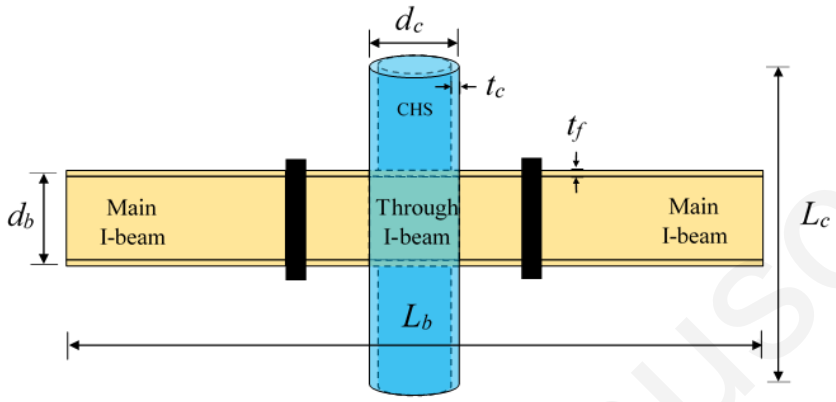

Fig. 3. *LASTEICON I-beam-to-CHS column connection with relevant geometric notations*

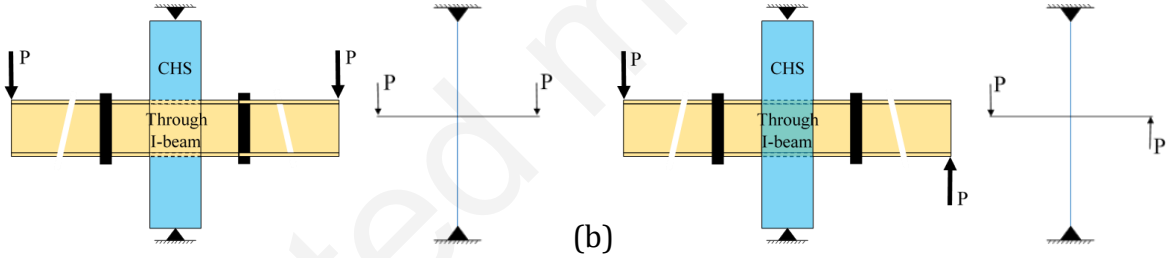

Fig. 4. *(a) LC1-Monotonic gravitational loading, (b) LC2-Monotonic opposite bending loading*

2.1. Design flexural strength of the LASTEICON connection

As the through members contribute significantly to the strength of the proposed LASTEICON "passing-through" connections, a different force-transfer mechanism was identified for each loading scenario, LC1 and LC2, in comparison with unstiffened and conventionally welded I-beam-to-CHS connections.

2.1.1 LC1: Monotonic gravitational loading

Under a gravitational or symmetric loading, the moments developed at either face of the CHS column connection ($M_{b,sym}$) cancel each other out (Fig. 5a) leading to a 'rigid body' like behavior of the joint. As a result, the resistance of the joint depends solely on the flexural resistance of the through I-beam just outside the CHS column. Therefore,

$$M_{b,Rd,sym} = M_{pl,Rd,beam} \quad (1)$$

Where, $M_{b,Rd,sym}$ is the joint flexural strength under symmetric loading, $M_{pl,Rd,Beam} = \frac{W_{pl} f_{yb}}{\gamma_{M0}}$, is the flexural resistance of the I-beam section obtained from EN 1993-1-1 [26], W_{pl} is the plastic section modulus of the I-beam, f_{yb} is the material yield stress of the I-beam, and γ_{M0} is the partial safety factor for cross section resistance. In order to reflect the nominal predicted strength and allow a direct comparison between the numerical and experimental outcomes, γ_{M0} was taken as 1 for the analytical calculations.

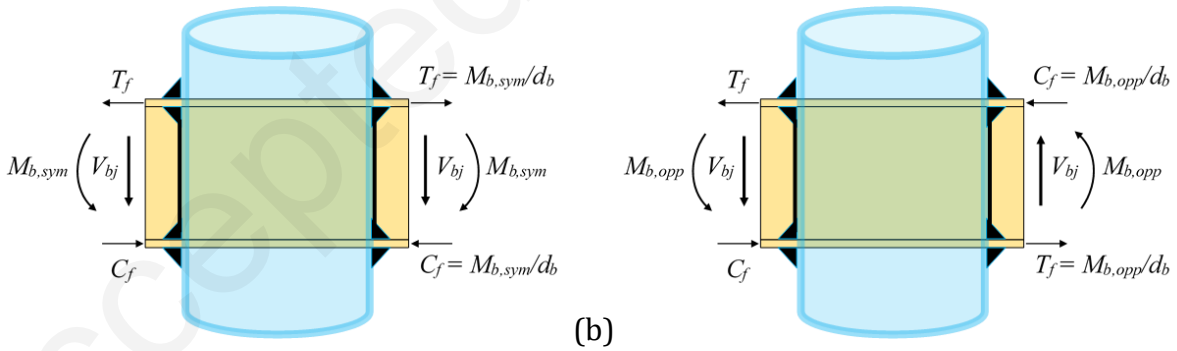

Fig. 5. *(a) Schematic diagram of forces acting at the joint panel under symmetric loading (LC1) (b) Schematic diagram of forces acting at the joint panel under antisymmetric loading (LC2)*

2.1.2 LC2: Monotonic opposite bending loading

Under an opposite or antisymmetric loading condition (Fig. 4b), the moment transfer mechanism could be visualized from the free body diagram illustrated in Fig. 5b. The beam moment demand can be resolved into flange forces, tensile force in the beam flange, T_f and compressive force in the beam flanges, C_f. Assuming that the bending moment is carried entirely by the furthest fibers of the flanges, the tensile and compressive forces in the beam flange, T_f and C_f, can be estimated as:

$$T_f = C_f = \frac{M_{b,opp}}{d_b} \quad (2)$$

Where, $M_{b,opp}$ is the moment demand at either side of the connection due to opposite bending loading and d_b is the total depth of the beam (Fig. 3a). The column shear (V_c) transferred through the joint increases the joint shear strength by reducing the beam flange forces transferred to the joint. As a result, the effective horizontal shear force acting on the joint panel, V_u, can be written as,

$$V_u = \frac{2M_{b,opp}}{d_b} - V_c \quad (3)$$

The numerical studies (discussed in Sections 3 and 4) showed that the beam flange forces and column shear transferred through the joint produce large shear forces in the through I-beam web as well as a substantial amount of transverse tensile and compressive forces on the CHS chord face at the flange connection zones. The newly proposed design procedure was therefore developed based on the shear resistance of the through I-beam web and the transverse tensile/compressive resistance offered by the CHS chord face. Fig. 6 shows an isolated portion of the top flange within the connection panel where the axial flange forces, T_f and C_f, tend to push the beam flange through the column. From the equilibrium of the

horizontal forces shown in Fig. 6, the horizontal shear force in the joint is resisted by the shear strength of the I-beam web, V_{wn}, and the in-plane design moment resistance of the CHS column wall, $M_{ip,1,Rd}$, which is defined according to EN 1993-1-8, Table 7.4 for X-type joints [27] and is derived from the transverse tensile/compressive resistance of the CHS chord face, $N_{1,Rd}$. However, as $M_{ip,1,Rd}$ was recommended for the Branch-type (conventional) connections, the calculated values were doubled to associate the increased resistance provided by the passing through elements as suggested by the latest draft of EN 1993-1-8, Table 9.4 [28] for passing through connections. Compared to the conventional connections where only the outer wall of the CHS column provides the resistance against transverse tensile or compressive forces, it can be observed through the LASTEICON connections that, the inner wall also offers resistance through the passing through elements therefore doubling the resistance of this connection.

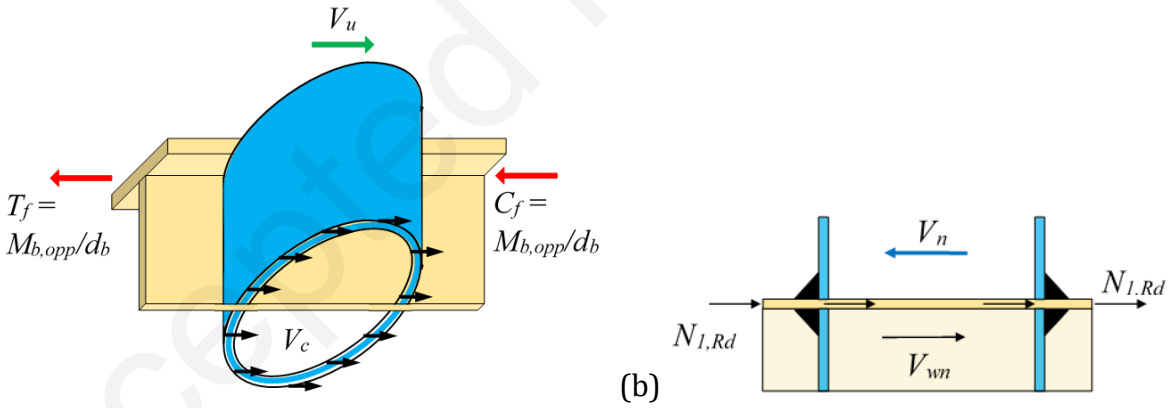

Fig. 6. *(a) Horizontal forces acting at the joint under opposite bending loading (LC2),* (b) *2D view of the passing through flange plates inside the CHS column illustrating the active resistances*

The complete joint shear capacity is reached when all the contributing mechanisms have reached their individual shear strengths. Thus, the total joint resistance, V_n, is calculated as the sum of the individual nominal shear strengths of the contributing mechanisms (Eq. 4).

$$V_n = (V_{wn} + V_{cn}) \quad (4)$$

Where,

$$V_{wn} = 0.6 f_{yw} d_c t_w \quad (5)$$

$$V_{cn} = \frac{M_{ip,1,Rd}}{d_b} \quad (6)$$

f_{yw} is the material yield stress for the I-beam web and t_w is the thickness of the I-beam web. The web shear yield is calculated based on an average yield shear stress of $0.6f_{yw}$ acting over the web area within the joint panel. The corresponding safety factors (γ_{M0} and γ_{M5}) in Eqs. 5 and 6 respectively, was taken as 1 for the analytical calculations to reflect on the nominal predicted strength. Therefore, the flexural resistance of the LASTEICON joint can be calculated as,

$$M_{b,Rd,opp} = (V_n + V_c)\frac{d_b}{2} \quad (7)$$

2.1.3 Checks for additional failure modes

Aside than the flexural failure of the joint, three additional failure modes can occur as local distortions due to the bending forces. In order to avoid such undesired failure at the joint, three checks are needed which are described below. However, as the joint shows a rigid like behaviour under the gravitational loading, LC1, these checks are only necessary for LC2.

Check 1: Check for flexural resistance of main beams:

For smaller sections, the through member might prove to be weaker than the joint panel and can thus lead to failure of the whole system due to flexural plasticity just outside the CHS column. To avoid such kind of a failure,

$$M_{b,Rd,opp} < M_{pl,Rd,Beam} \quad (8)$$

Where, $M_{pl,Rd,Beam} = \frac{W_{pl} f_{yb}}{\gamma_{m0}}$, is the flexural resistance of the I-beam section [26].

Check 2: Check for local buckling of CHS column:

Conditions to avoid premature local buckling are described below. Firstly, the CHS column sections should be classified according to Table 5.2 of EN 1993-1-1 based on the diameter-to-thickness ratio of the CHS. Now, as Class 3 and Class 4 hollow sections are deemed susceptible to local buckling [29], their flexure resistance, $M_{Rd,CHS}$, is derived from the following equations.

For Class 3 sections: $M_{Rd,CHS} = \frac{W_{el,CHS} f_{yc}}{\gamma_{m0}}$ (9)

For Class 4 sections: $M_{Rd,CHS} = \frac{W_{eff,CHS} f_{yc}}{\gamma_{m0}}$ (10)

Where, f_{yc} is the material yield stress for the CHS column, $W_{el,CHS}$ and $W_{eff,CHS}$ are respectively defined as the elastic section modulus and effective section modulus of the CHS according to EN 1993-1-1. To avoid a failure due to local buckling of the CHS,

$$M_{b,Rd,opp} < M_{Rd,CHS} \frac{(L_b - d_c) L_c}{(L_c - d_b) L_b} \quad (11)$$

Where, L_b is the total length of the beam, d_c is the external diameter of the CHS column, and L_c is the total length of the CHS column as shown in Fig. 3a. It is recommended to avoid slender CHS columns (Class 3 and Class 4 hollow sections) in the LASTEICON joints. This can be done

simply by using the first step of this design check i.e. classification according to the EN 1993-1-1.

Check 3: Check for punching shear failure:

A further check is also suggested for the conventional I-beam-to-CHS joints as specified in EN 1993-1-8 [27] and CIDECT guidelines [8] to avoid punching shear failure. This check is also included for these LASTEICON joints to offer additional safety. According to the available design guidelines, the check is only needed if,

$$b \leq d_c - 2t_c \tag{12}$$

and if required, the following restriction should be respected.

$$f_b t_f \leq 1.16 f_{yc} t_c \tag{13}$$

Where, b is the through I-beam flange width, t_c is the CHS thickness, t_f is the I-beam flange thickness and f_b is the stress at which punching shear occurs on the CHS column wall. Therefore, as f_b is induced due to the bending moment, M_{bp},

$$M_{bp} = f_b W_{el,beam} \tag{14}$$

Where $W_{el,beam}$ is the elastic section modulus of the through I-beam. Therefore, to avoid failure due to punching shear in the CHS column wall,

$$M_{b,Rd,opp} < M_{bp} \tag{15}$$

2.1.4 Correlation to the global configuration

The above-mentioned design procedure determines the resistance of the passing through joint from a local perspective. However, in order to correlate the design procedure to the numerical and experimental prototypes and further compare the analytical results with the

numerical simulations, the joint strengths should be calculated in terms of the shear force developed due to the vertical loads acting at the extremities of the main I-beams. Therefore, if P is the vertical load at the free end of the main I-beam and V_{bj} is the corresponding shear developed on the beam at the location of the CHS column face (Fig. 5),

$$P = V_{bj} = \frac{M_b}{(L_b - d_c)/2} \tag{16}$$

Where, M_b is equal to $M_{b,sym}$ under LC1 and $M_{b,opp}$ under LC2. In the through beam connection detail, it is reasonable to consider that the entire column shear force is effectively reducing joint shear forces since the column is continuous through the joint and is directly attached to the beam through proper welds. This makes the joint strength dependent on the global configuration and the column shear (V_c), which can be calculated from,

$$V_c = P\frac{L_b}{L_c} = \frac{M_b}{(L_b - d_c)}\frac{2L_b}{L_c} \tag{17}$$

Therefore, the joint strength derived in Eq. 7 can be rewritten as,

$$M_{b,Rd,opp} = \frac{(V_{wn} + V_{cn})}{\left[\frac{2}{d_b} - \frac{2L_b}{L_c}\left(\frac{1}{L_b - d_c}\right)\right]} \tag{18}$$

Furthermore, it can be derived in terms of V_{bj} following Eq. 16. Similar expressions were also derived in terms of shear corresponding to the moments for all three checks. Therefore, Eqs. 8, 11 and 15 can be rewritten as,

$$V_{bj}\left(= \frac{M_{b,Rd,opp}}{(L_b - d_c)/2}\right) < V_{bb}\left(= \frac{M_{pl,Rd,Beam}}{(L_b - d_c)/2}\right) \tag{19}$$

$$V_{bj}\left(= \frac{M_{b,Rd,opp}}{(L_b - d_c)/2}\right) < V_{bc}\left(= \frac{M_{Rd,CHS}}{(L_c - d_b)/2}\left(\frac{L_c}{L_b}\right)\right) \tag{20}$$

$$V_{bj}\left(= \frac{M_{b,Rd,opp}}{(L_b - d_c)/2}\right) < V_{bp}\left(= \frac{M_{bp}}{(L_b - d_c)/2}\right) \tag{21}$$

As a detailed parametric study is presented in this investigation, the minimum value of all four V_b values is considered as the shear force corresponding to the ultimate strength of the LASTEICON joint. Therefore, to identify the probable failure mode, $V_{bu,opp}$ is taken as,

$$V_{bu,opp} = min(V_{bj}, V_{bb}, V_{bc}, V_{bp}) \quad (22)$$

2.2 Design shear strength of the LASTEICON connection

The shear strength of the "passing-through" joint can be determined from the shear strength of the through I-beam. According to EN 1993-1-1, Clause 6.2.6, it can be calculated as,

$$V_{joint} = V_{pl,Rd,beam} = \frac{A_{vb} f_{yb}}{\sqrt{3}\gamma_{m0}} \quad (23)$$

Where, A_{vb} is the shear area of the through I-beam.

Table 1 lists all the parametric variations along with their ultimate flexural and shear strength of the joint calculated according to this design procedure. Values corresponding to all three checks are also provided to show the failure predictions made by the proposed design procedure.

Table 1: Analytical values corresponding to the joint strength, $M_{b,Rd,opp}$ and V_{bj}, all three checks, V_{bb}, V_{bc} and V_{bp} and ultimate joint strength, $V_{bu,opp}$[2]

Varying Parameters	Joint Flexural Strength		Joint Shear Strength	Check 1: Beam plasticity	Check 2: Local buckling	Check 3: Punching shear			Joint Ultimate Strength	Failure Modes
	$M_{b,Rd,opp}$ (kNm)	V_{bj} (kN)	V_{joint} (kN)	V_{bb} (kN)	V_{bc} (kN)	f_b (MPa)	M_{bp} (kNm)	V_{bp} (kN)	$V_{bu,opp}$ (kN)	
For Beam Section variation (IPE)										
IPE 220	116.3	50.1	325.9	43.6	198.9	475.3	119.8	51.6	43.6	Beam Flexure
IPE 270	161.0	69.3	453.0	74.0	203.7	428.7	183.9	79.2	69.3	Joint Panel Shear
IPE 330	225.9	97.3	631.3	122.9	209.7	380.3	271.1	116.8	97.3	Joint Panel Shear
IPE 400	316.3	136.2	875.2	199.8	217.3	323.9	375.8	161.8	136.2	Joint Panel Shear
IPE 500	475.7	204.8	1227.7	335.4	229.1	273.3	527.5	227.2	204.8	Joint Panel Shear
For CHS Thickness variation (t_c)										
4.0	184.7	79.5	875.2	199.8	69.9	129.6	150.3	64.7	64.7	CHS Punching
6.0	216.0	93.0	875.2	199.8	103.0	194.4	225.5	97.1	93.0	Joint Panel Shear
8.0	259.9	111.9	875.2	199.8	135.1	259.2	300.6	129.5	111.9	Joint Panel Shear
10.0	316.3	136.2	875.2	199.8	217.3	323.9	375.8	161.8	136.2	Joint Panel Shear
12.5	404.4	174.1	875.2	199.8	267.8	404.9	469.7	202.3	174.1	Joint Panel Shear
For CHS Diameter variation (d_c)										
273.0	319.6	135.2	875.2	196.3	125.9	323.9	375.8	159.0	125.9	Local Buckling
323.9	313.0	133.9	875.2	198.4	179.3	323.9	375.8	160.7	133.9	Joint Panel Shear
355.6	316.3	136.2	875.2	199.8	217.3	323.9	375.8	161.8	136.2	Joint Panel Shear
406.4	327.4	142.5	875.2	202.0	285.9	323.9	375.8	163.6	142.5	Joint Panel Shear
457.0	342.6	150.8	875.2	204.3	279.3	323.9	375.8	165.4	150.8	Joint Panel Shear

[2] Reference configuration chosen for parametric studies: IPE400 section passing through a CHS column with diameter, d_c = 355.6 mm and thickness, t_c = 10.0 mm, total column length, L_c = 2340.0 mm, total beam length, L_b = 5000 mm, material yield strength for the beams, f_{yb} = 355 Mpa, and CHS columns, f_{yc} = 377 Mpa, and IPE 400 as the "main" I-beam sections.

334 **Table 1:** Analytical values corresponding to the joint strength, $M_{b,Rd,opp}$ and V_{bj}, all three checks, V_{bb}, V_{bc} and V_{bp} and ultimate joint

335 strength, $V_{bu,opp}$[3] (continued..)

Varying Parameters	Joint Flexural Strength		Joint Shear Strength	Check 1: Beam plasticity	Check 2: Local buckling	Check 3: Punching shear			Joint Ultimate Strength	Failure Modes
	$M_{b,Rd,opp}$ (kNm)	V_{bj} (kN)	V_{joint} (kN)	V_{bb} (kN)	V_{bc} (kN)	f_b (MPa)	M_{bp} (kNm)	V_{bp} (kN)	$V_{bu,opp}$ (kN)	
For CHS and Beam Material variation (f_{yc} & f_{yb})										
275.0 & 275.0	237.9	102.5	678.0	154.8	158.5	236.3	274.1	118.0	102.5	Joint Panel Shear
355.0 & 355.0	307.1	132.3	875.2	199.8	204.6	305.0	353.8	152.4	132.3	Joint Panel Shear
440.0 & 440.0	380.7	163.9	1084.7	247.6	253.6	378.1	438.6	188.9	163.9	Joint Panel Shear
355.0 & 377.0	316.3	136.2	875.2	199.8	217.3	323.9	375.8	161.8	136.2	Joint Panel Shear
355.0 & 440.0	342.5	147.5	875.2	199.8	253.6	378.1	438.6	188.9	147.5	Joint Panel Shear
440.0 & 355.0	345.4	148.7	1084.7	247.6	204.6	305.0	353.8	152.4	148.7	Joint Panel Shear
For varying Moment-to-shear (M/V) ratio by varying beam length (L_b)										
2500.0	322.3	300.6	875.2	432.7	434.6	323.9	375.8	350.5	300.6	Joint Panel Shear
3400.0	319.0	209.5	875.2	304.8	319.6	323.9	375.8	246.9	209.5	Joint Panel Shear
5000.0	316.3	136.2	875.2	199.8	217.3	323.9	375.8	161.8	136.2	Joint Panel Shear
6600.0	315.0	100.9	875.2	148.6	164.6	323.9	375.8	120.4	100.9	Joint Panel Shear
7500.0	314.5	88.0	875.2	129.9	144.9	323.9	375.8	105.2	88.0	Joint Panel Shear

336

[3] Reference configuration chosen for parametric studies: IPE400 section passing through a CHS column with diameter, d_c = 355.6 mm and thickness, t_c = 10.0 mm, total column length, L_c = 2340.0 mm, total beam length, L_b = 5000 mm, material yield strength for the beams, f_{yb} = 355 Mpa, and CHS columns, f_{yc} = 377 Mpa, and IPE 400 as the "main" I-beam sections.

3. MODELLING APPROACH AND EXPERIMENTAL VALIDATION OF THE NUMERICAL MODELS

This section presents the modelling techniques adopted to build the numerical prototypes in the finite element software DIANA 10.2 [30] and discusses their validation with respect to the relevant experimental investigations obtained in the LASTEICON project.

Modelling assumptions and Finite Element (FE) models

The configurations were modelled using 3D geometries and solid elements such as CHX60, CTP45 and CTE30 [31]. The laser cut slots on the CHS column surface were taken into account to allocate the through I-beam and allow for the necessary reduction in CHS stiffness. As mentioned in Section 2, to avoid any secondary connection failure and rather focus on the I-beam-to-CHS "passing-through" zone, the slots in the FE models were defined assuming a zero spacing tolerance, thus connecting the CHS column and the "through" beam with a perfectly welded connection. To avoid heavy and complicated numerical models and save computation time, welds were not modelled explicitly and the members were connected through common nodes. Fig. 7 shows some illustrations of the numerical model. Two different load cases were considered where both vertical loads were incremented simultaneously in each analysis step. Geometric nonlinearity was considered in the numerical simulations. Material nonlinearity was introduced in the models through actual stress strain relationships obtained from the coupon tests on the experimental prototypes. The material yield strength for the I-beam, f_{yb}, and for the CHS column, f_{yc}, was found to be 355MPa and 377MPa respectively. Furthermore, in-built material models in DIANA 10.2

were used according to Table 3.1 (EN 10025-2), EN 1993-1-1, to compare the variations in the connection behaviour due to different steel grades, when used for either the CHS column or the through beams.

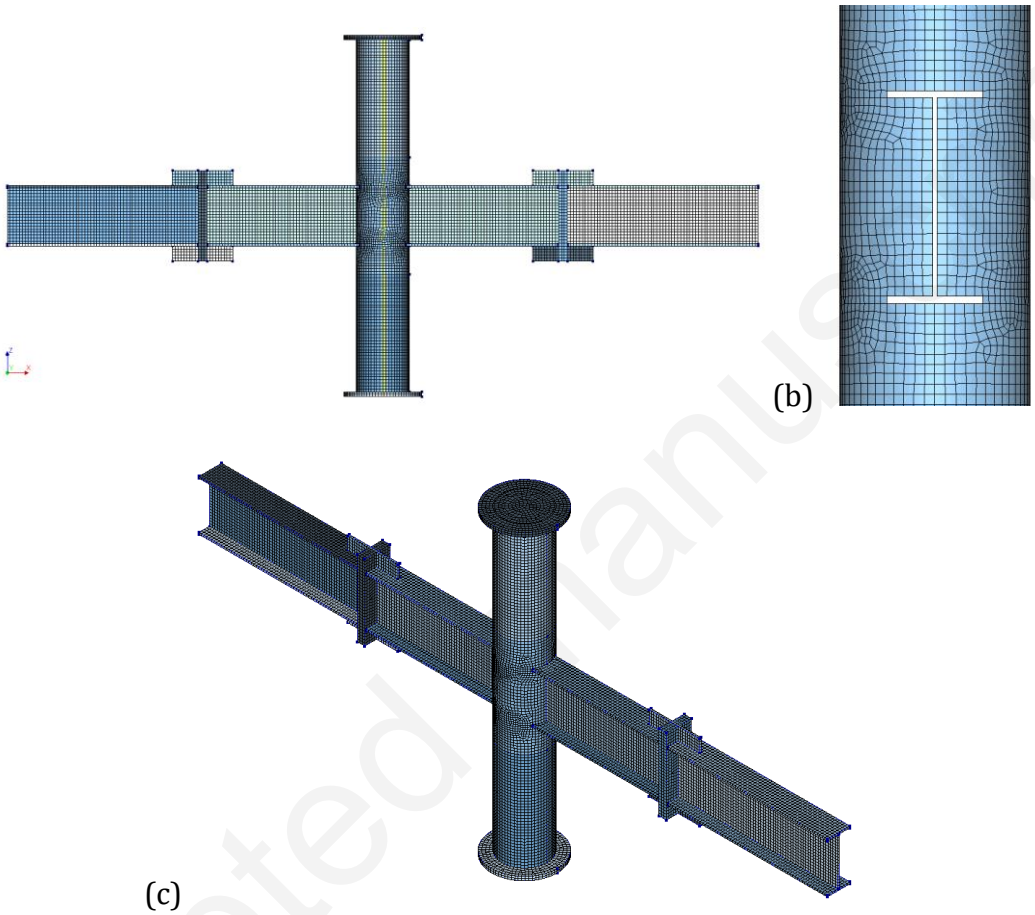

Fig. 7. *Examples of the numerical model meshed in DIANA 10.2, (a) frontal view of the complete connection configuration, (b) slots on the CHS column to accommodate the through beam, (c) isometric view of the configuration.*

Experimental Validation of the Numerical FE Models

A preliminary experimental campaign was conducted by INSA, Rennes [32] to validate the numerical model for both load cases. Two additional solid circular plates, with 30 mm thickness and 520 mm diameter, were connected to each extremity of the CHS column and

was pinned by rollers following the boundary conditions shown in Fig. 4. Bracings were placed to limit the lateral torsional buckling of the beam. These additional plates and bracings were also considered in the numerical models to have an exact replica of the experimental specimens and thus provide an appropriate validation. Further details about the test set-up can be found in the LASTEICON experimental report provided by INSA, Rennes [32]. Two load-jacks of 1500 KN capacity, were applied at the extremities of the main beams at a distance of 2500 mm from the axis of the CHS column for LC1. This distance was reduced to 1700mm for LC2 to allow for a larger rotation of the node (joint panel) at failure. The monotonic loadings were applied in three steps: (i) Application of 50% of the theoretical design resistance evaluated with nominal mechanical characteristics, and unloading, (ii) Application of 100% of the design resistance and unloading, and finally (iii) Loading until failure of the joint or the beam. Inclinometers and LVDTs were placed in necessary locations to measure the vertical and horizontal displacements at specific positions of the joint configuration. Three specific connection configurations (see Table 2) were investigated in the experimental campaign: two different passing-through LASTEICON connection configurations (one for each load case, LC1 and LC2) and one conventional I-beam-to-CHS connection configuration (Fig. 8) under LC1 without any "passing-through" mechanism. The beams were directly welded to the CHS column surface for the third test (i.e. the conventional configuration). Experimental and numerical results were compared through force-displacement curves (for an extremity of the beam, where the vertical force is increased systematically) and failure modes. The material stress-strain curves obtained from the coupon tests (and adopted for the numerical models) are plotted in Fig. 9a. Very good agreement was found between the experimental (_Exp.) and numerical (_Num.) results in

terms of initial stiffness and ultimate resistance of the LASTEICON as well as the conventional joints as shown in Fig. 9b.

The experiments regarding LASTEICON_LC1 and Conventional_LC1, characterized by a very ductile behaviour, were stopped at an arbitrary point before reaching the displacement capacity of the loading system. A similar approach was followed for the numerical models for these two cases, i.e. the numerical simulations were stopped when the displacement was found as large enough to get relevant and useful information on the behaviour of the joint. On the other hand, the experiment regarding LASTEICON_LC2 failed in a less ductile manner due to damage in the connection zone (tearing of the CHS column surface) between the through I-beam flange and the CHS column. To identify "failure" in the numerical FE-models, the accumulated plastic strains were compared to a limit value, which were calibrated by the test results. A similar approach has been used in different research studies [18, 33] to validate the numerical models against experimental results. For each tested specimen and its corresponding FE-model, the location and the values of the accumulated plastic strains were determined from the simulations at the deformation stage of the tested specimen corresponding to the first visually detected failure (i.e. I-beam flange plasticity in case of LASTEICON_LC1, CHS wall tearing in case of LASTEICON_LC2 and CHS wall crushing in case of Conventional_LC1). For this particular study, the limit value for equivalent plastic strain was considered equal to 6.5%.

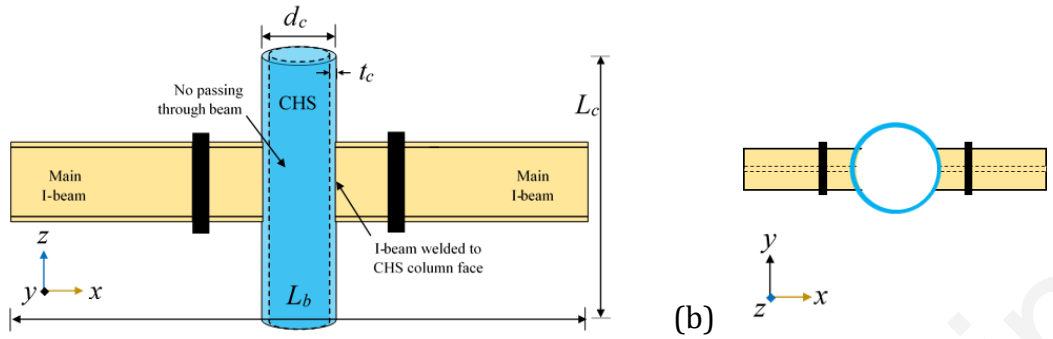

Fig. 8. *Schematic diagram of a conventional open-to-CHS connection (a) frontal view and (b) top view*

Table 2: Specimens tested in the Preliminary Experimental Campaign

Configuration Type	*Loading Scenario*	*Specimen Name*	*Beam* (IPE)	L_b (mm)	d_c (mm)	t_c (mm)	L_c (mm)
LASTEICON	LC1	LASTEICON_LC1	IPE 400	5000.0	355.6	8.8	2340.0
LASTEICON	LC2	LASTEICON_LC2	IPE 400	3400.0	355.6	10.0	2340.0
Conventional	LC1	Conventional_LC1	IPE 400	5000.0	355.6	10.0	2340.0

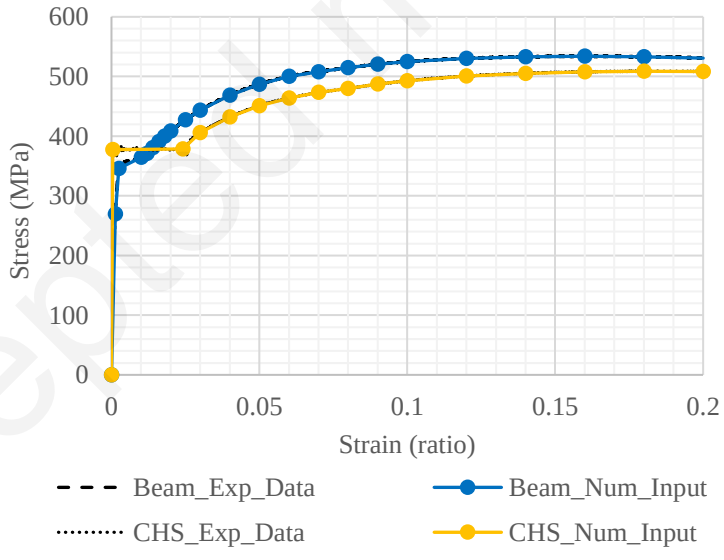

(a)

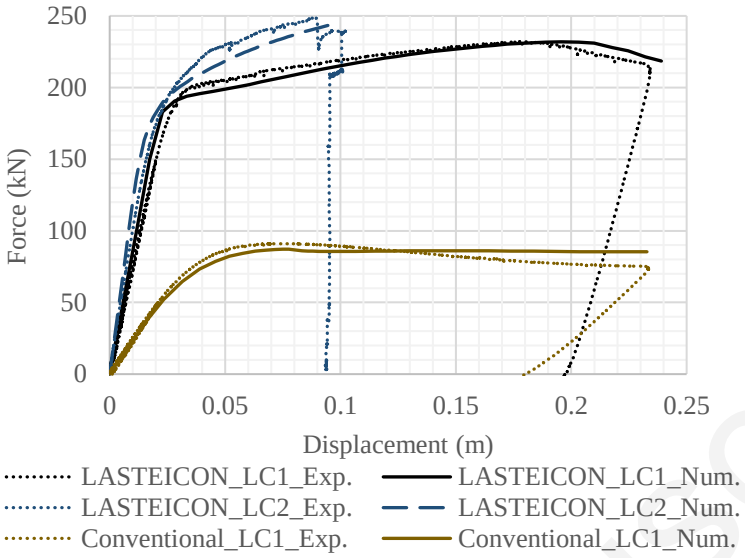

(b)

Fig. 9. *(a) Actual stress-strain relationship obtained for S355 from the experimental tests, (b) comparison of force-displacement curves between numerical and experimental results*

(a)

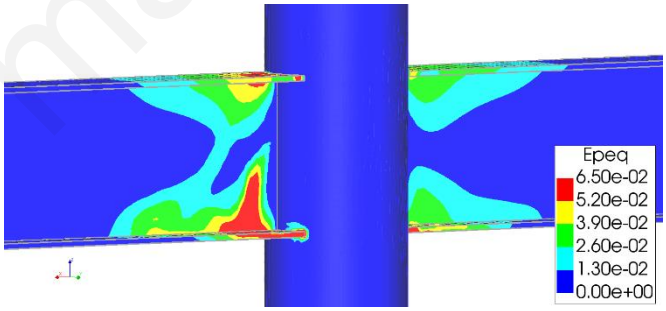

(b)

Fig. 10. *LASTEICON_LC1 Failure: (a) flange buckling of beam flanges in compression observed from experiments, (b) von Mises equivalent plastic strains in the numerical model*

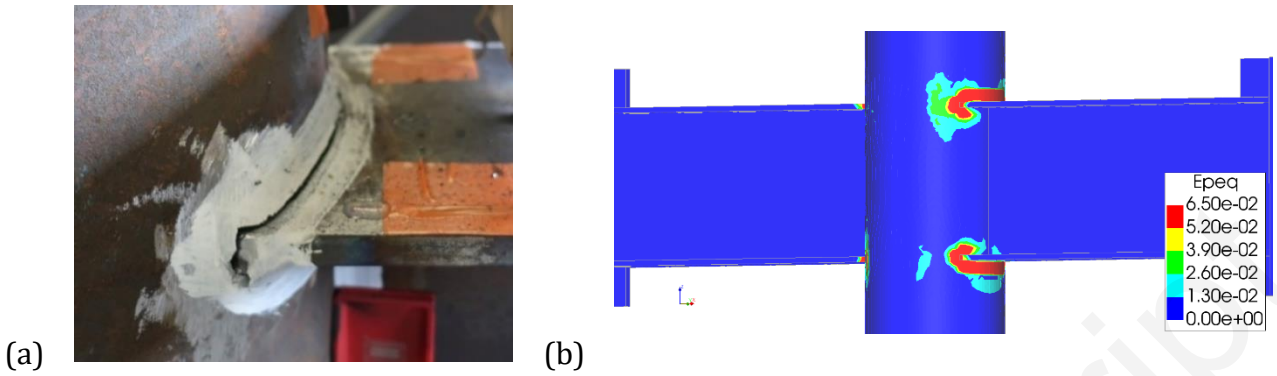

Fig. 11. *LASTEICON_LC2 Failure: (a) beam-to-column connection tearing observed from experiments, (b) von Mises equivalent plastic strains in the numerical model*

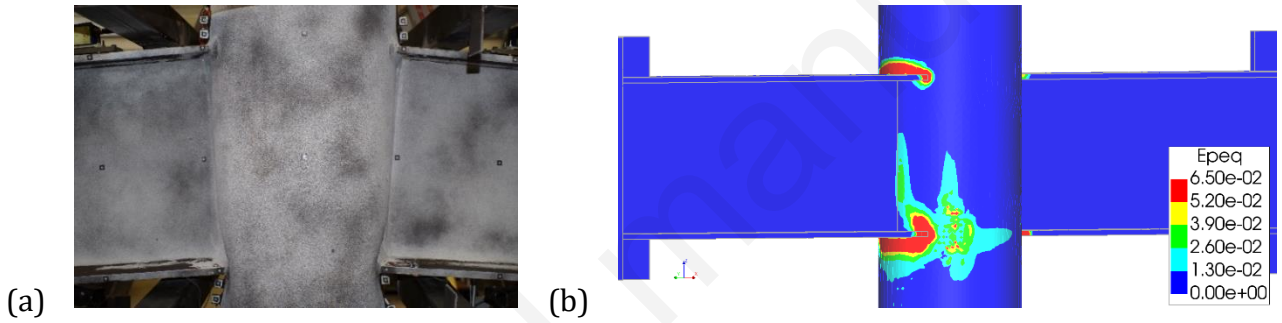

Fig. 12. *Conventional_LC1 Failure: (a) CHS column surface in compression observed from experiments, (b) von Mises equivalent plastic strains in the numerical model*

Similar failure modes were obtained from the numerical and experimental studies for all three configurations (Fig. 10-12). The failure due to beam flange plasticity is clearly visible for the LASTEICON_LC1 specimen, where the buckled I-beam flanges of the experimental prototype (Fig. 10a) validates the strain concentration (Fig. 10b) on the I-beam flanges just outside the CHS column. Failure in the LASTEICON_LC2 specimen occurred due to a tearing of the CHS column surface at the connection zone between the CHS column and the through flanges (Fig. 11a). Similar failure behaviour was obtained in the numerical models as the

limiting plastic strains developed around the connection zone (Fig. 11b). This phenomenon however occurred due to a shear failure of the through I-beam web and transverse tensile failure of the CHS column wall. It is explained in Section 4 with more details. A good agreement was also obtained regarding the failure mode in the conventional joint configuration under LC1 (Fig. 12), as the CHS wall crushing under compression was emulated by the high plastic strain concentration on the CHS column wall at the I-beam-to-CHS connection zones in the numerical models.

4. PARAMETRIC STUDY ON THE LASTEICON CONFIGURATION BASED ON NONLINEAR STATIC ANALYSIS

Five parameters were principally identified to have a significant influence on the ultimate joint strength and were thus varied in this study. The chosen parameters are: (1) through I-beam section (*IPE*), (2) CHS column thickness (t_c), (3) CHS column diameter (d_c), (4) Material properties for both CHS and through I-beam (f_{yb} and f_{yc}), and (5) Moment-to-shear (M/V) ratio. The reference configuration, chosen as a starting point for the parametric study, consisted of an IPE400 section passing through a CHS column with 355.6mm diameter (d_c) and 10mm thickness (t_c) with a total beam length (L_b) of 5000mm (see Fig. 13). Results for this particular configuration is presented using a solid blue line in all the force-displacement plots. All the parametric studies, except the one related to material variation, were done with the experimental material properties (Fig. 9a).

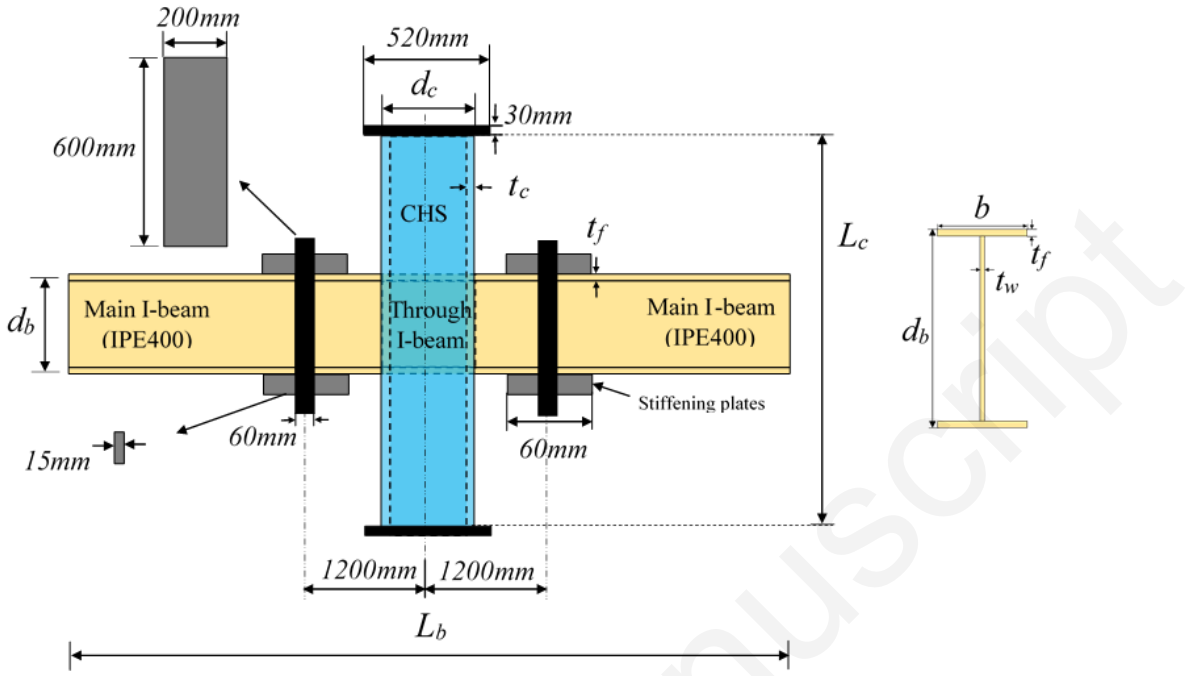

Fig. 13. *All parametric dimensions for the LASTEICON configuration*

Both the aforementioned load cases, LC1 (Fig. 4a) and LC2 (Fig. 4b), were considered for each parametric variation. The loads were applied to the extremities of the main I-beams and were incremented to obtain the force-displacement behaviour. The monitored displacement is measured at the loading point. The investigated variations for each parameter are listed in the left most column of Table 1 (in grey colour) with their ultimate joint strengths derived from the proposed design approach in Section 2. The resulting analytical values were compared with the numerical results. The dotted horizontal lines in the force-displacement curves under LC1 and LC2 corresponds to the V_{bb} and $V_{bu,opp}$ values listed in Table 1.

4.1 Through I-beam section (IPE)

The most important parameter influencing the ultimate joint strength was identified to be the through I-beam section. Five different IPE sections were chosen as listed in Table 1. Vertical force-displacement curves for the gravitational loading, LC1, and the opposite bending loading, LC2, are plotted in Fig. 14 and 15, respectively.

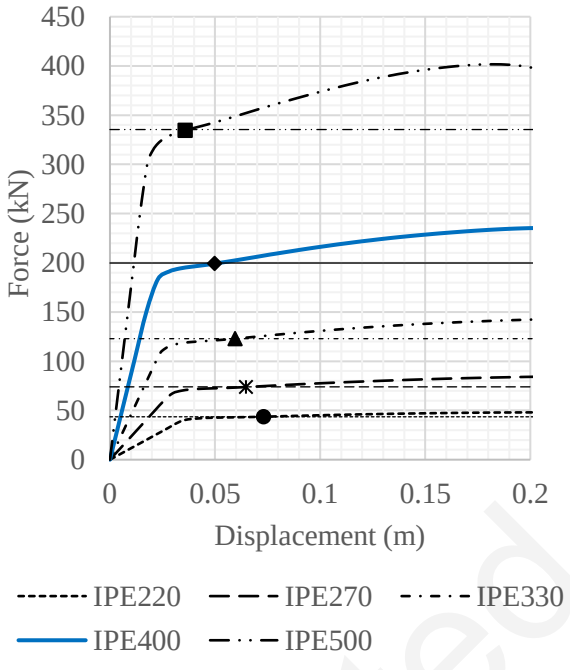

Fig. 14. *Vertical force-displacement curve comparisons for varying through IPE sections under LC1*

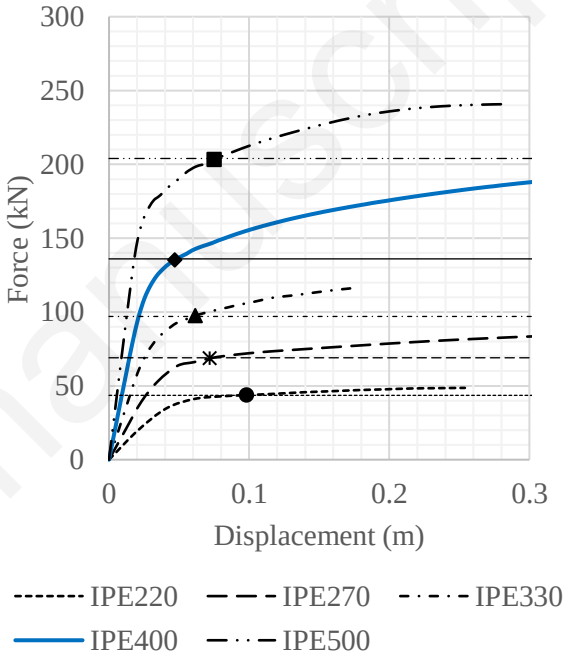

Fig. 15. *Vertical force-displacement curve comparisons for varying through IPE sections under LC2*

In the numerical models, failure was identified when the element strain reached the limiting value for the equivalent plastic strain obtained from the experiments (mentioned in section 3). For LC1, the failure was solely dominated by the flange plasticity of the through I-beam just outside the CHS column as shown in Fig. 16 in terms of von Mises stresses. The analytical values of the plastic flexural resistance of the through I-beams (V_{bb} corresponding to

$M_{pl,Rd,beam}$) were compared with the force-displacement curves obtained from the FE models. Larger sections provided a greater resistance beyond the analytical values compared to smaller sections. This occurred due to the higher moment-curvature offered by the larger sections through increasing the lever arm distance between their flanges. Von Mises stresses shown in Figures 16a and 16b illustrate the failure obtained in the LASTEICON configurations consisting of the weakest "through" I-beam - IPE220, and the strongest "through" I-beam - IPE500.

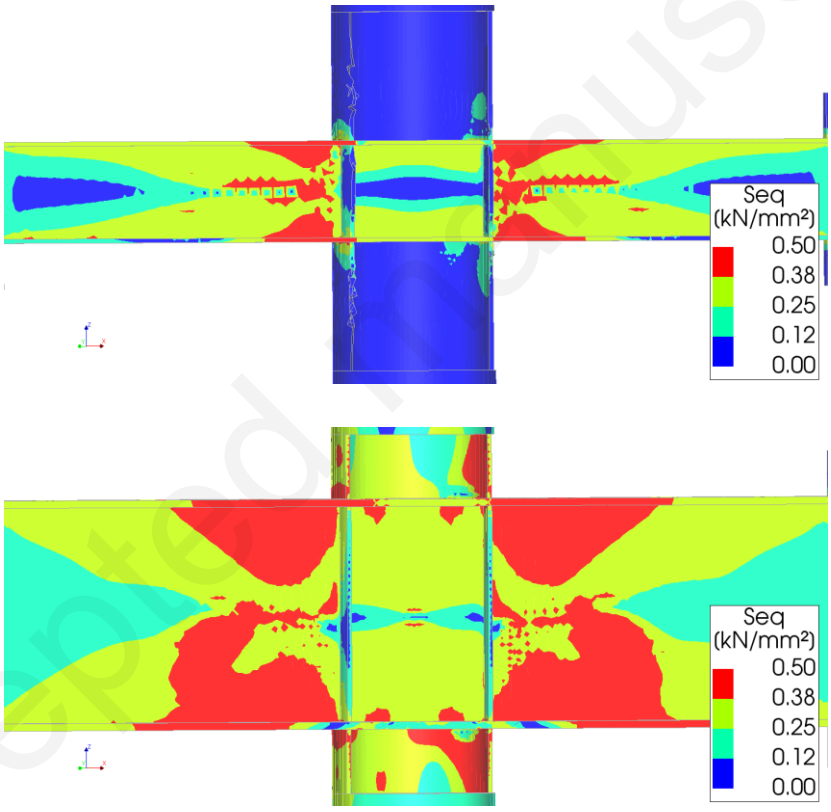

Fig. 16. *Von Mises equivalent stresses (kN/mm²) at failure under LC1 for configurations with (a) IPE220 through beam, (b) IPE500 through beam*

No variation was however noticed in the failure pattern. The flanges of the through IPE beams started to yield just outside the CHS column wall prior to all other components of the

connection. This occurred due to a rigid-body like behaviour of the main joint panel. Under LC1, both the moments nullify each other at the joint panel and do not contribute to the failure sequence. Therefore, failure is solely caused by flange plasticity of the through I-beam just outside the CHS column. The front half of the CHS column is removed from the figures to have a clear view of what is happening inside the "passing-through" connection zone.

A different force-transfer mechanism was observed under LC2 as both the through I-beam web and the CHS column surface contributed to the ultimate joint strength. Failure occurred simultaneously in both the through I-beam web and the CHS column surface. This strongly validated the proposed design approach, since an effective transmission of bending moments occurred through a combination of shear resistance provided by the through section and the transverse tensile/compressive resistance of the CHS chord face. The ultimate joint strengths, $V_{bu,opp}$ (see Table 1), are compared in Fig. 15 to highlight the agreement shared between the analytical and numerical results under LC2. For this load condition, the moment applied on the connection configurations is primarily resisted by the shear capacity of the through I-beam and is then transferred to the CHS column to utilize its transverse tensile/compressive resistance. Hence, if the through I-beam is not strong enough, it will be impossible to fully activate the CHS resistance. This phenomenon was identified using the LASTEICON configuration with a through IPE220, where failure occurred due to a beam flange plasticity outside the CHS column (Fig. 17a) prior to reaching the full capacity of the joint panel. No significant failure stresses were observed in the CHS column surface and the passing through I-beam web. A similar failure pattern was predicted by the analytical calculations presented in Table 1 ($V_{bb} < V_{bj}$). The necessity of the proposed Design Check 1 can therefore be substantiated.

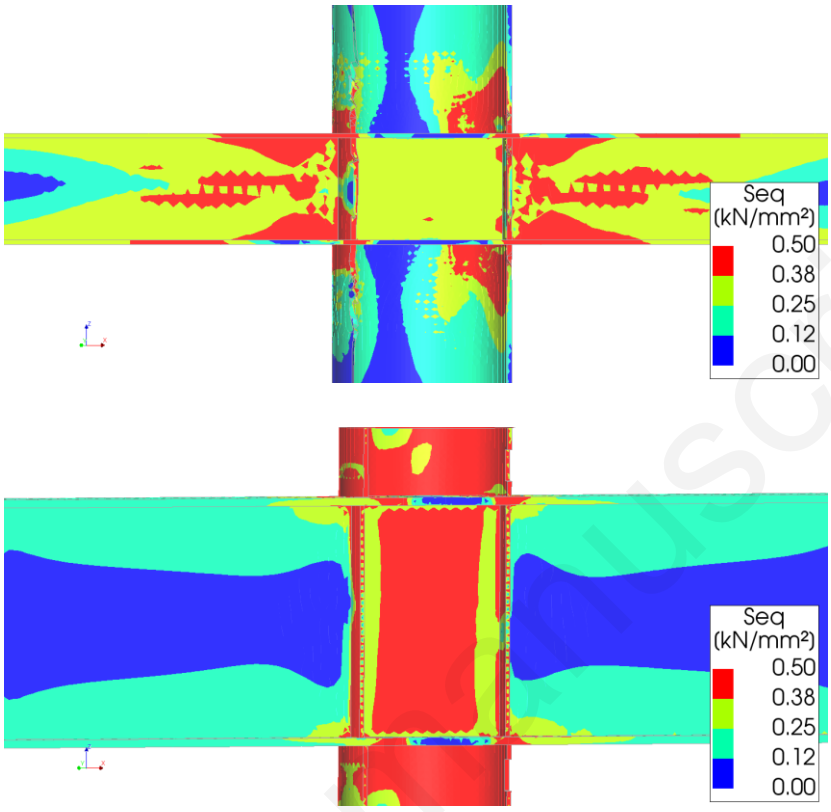

Fig. 17. *Von Mises equivalent stresses (kN/mm²) at failure under LC2 for configurations with (a) IPE220 through beam, (b) IPE500 through beam*

On the contrary, failure in the other configurations occurred due to a failure of the complete joint panel as predicted by the analytical design calculations. Maximum failure stresses were obtained at the faces of the CHS column at the flange connection zones as well as the through I-beam web as shown in Fig. 17b. The failure stresses developing at the connection zone of the CHS column clearly explained the tearing observed in the experimental prototype (Fig. 11) and confirmed that it occurred due to an ultimate joint failure rather than any localized distortion of the CHS column wall, hence validating the benefits anticipated for the "passing-through" LASTEICON connections.

4.2 CHS column thickness (t_c)

The CHS column thickness was varied from a smallest of 4 mm to a largest of 12.5 mm (Table 1) to understand all possible failure sequences occurring due to any localized failure in the CHS column. Force-displacement curves, for LC1 and LC2, are shown in Fig. 18 and 19 respectively for the CHS thickness variation.

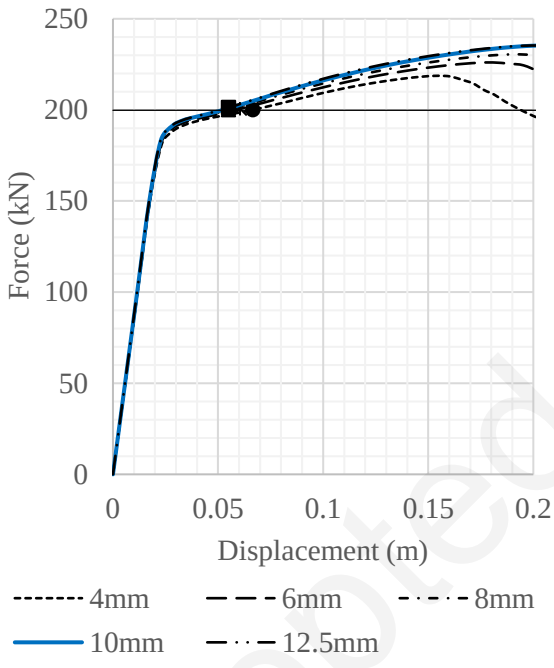

Fig. 18. *Vertical force-displacement curve comparisons for varying CHS column thickness under LC1*

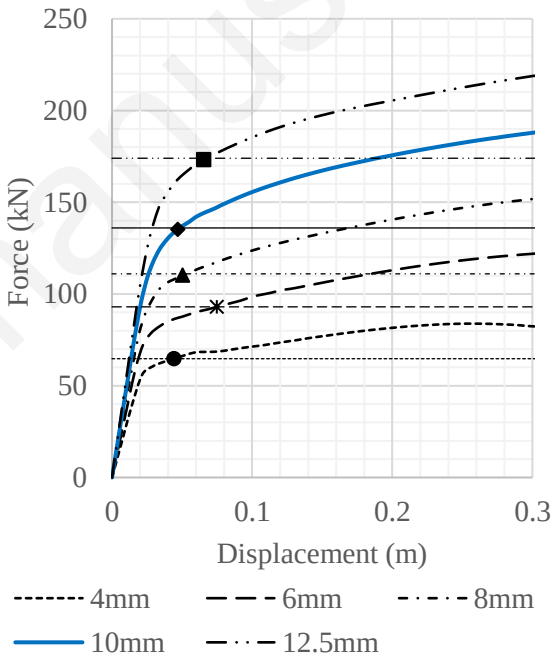

Fig. 19. *Vertical force-displacement curve comparisons for varying CHS column thickness under LC2*

As the failure under LC1 is solely dominated by the flange buckling of the through I-beam and the I-beam section was kept constant in this subsection, varying CHS column thickness did not have any effect on the numerical models (Table 1, Fig. 18 and Fig. 20). Therefore, the

analytical value (V_{bb} corresponding to $M_{pl,Rd,beam}$) of IPE 400 was compared with the force-displacement curves. A thicker CHS was however observed to provide a slightly larger resistance and ductility due to an increased overlapping and thus overstrengthening of the "passing-through" connection zone. When the thickness was reduced to 4 mm, the CHS column could not provide such amount of rigidity and therefore, some stress concentrations were observed in the through flanges inside the CHS column as shown in Fig. 20a. Nevertheless, the failure pattern remained unaffected for all configurations.

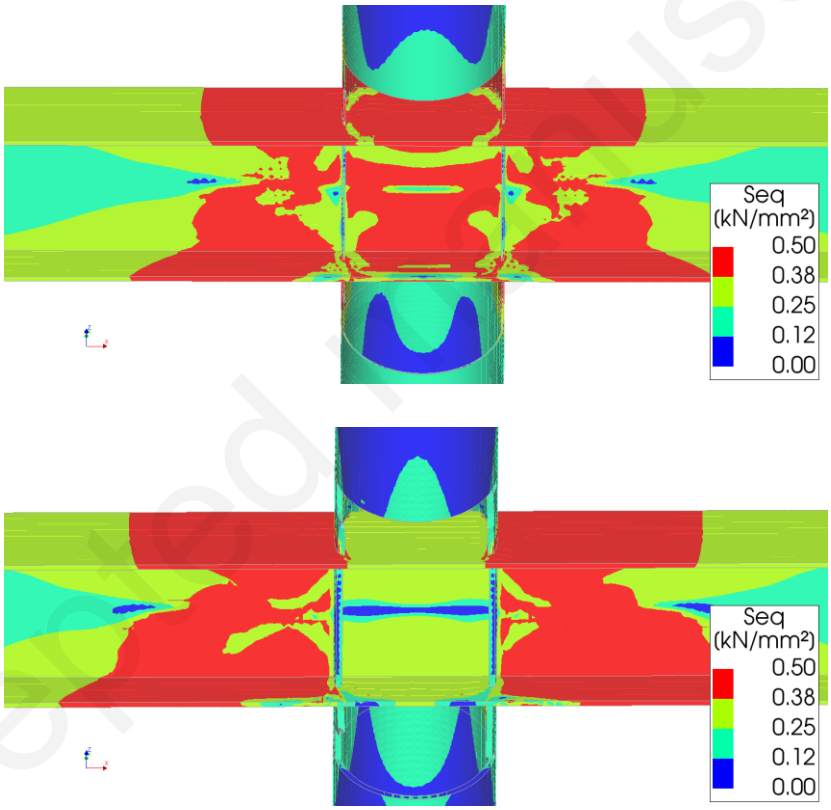

Fig. 20. *Von Mises equivalent stresses (kN/mm²) at failure under LC1 for configurations with (a) 4mm thick CHS, (b) 12.5mm thick CHS*

The CHS column thickness has, however, a substantial effect in the force-displacement behaviour as well as the failure mode of the joint configuration under LC2. As listed in Table

1, the failure mode changed from a punching shear failure for the thinner columns (Class 4 sections) to an ultimate joint panel failure for the thicker columns. Although the 6 mm thick CHS column was calculated as a Class 4 section, it was close to the Class 3 limit and therefore, offered a punching shear resistance marginally higher than the actual joint strength (also see Table 1). The ultimate joint strengths calculated as per Table 1 are further compared in Fig. 19 to highlight the agreement shared between the analytical and numerical resistances.

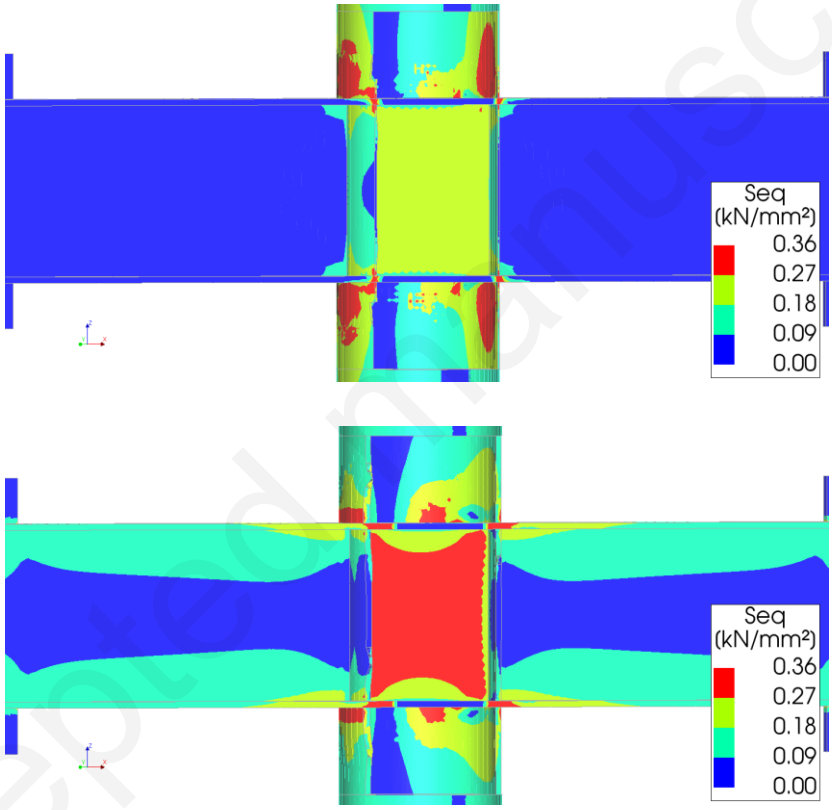

(a)

(b)

Fig. 21. *Von Mises equivalent stresses (kN/mm²) at yield under LC2 for configurations with (a) 4mm thick CHS, (b) 12.5mm thick CHS*

As suggested by the analytical calculations in Section 2, slender CHS columns, specifically belonging to Class 4, are susceptible to local buckling as well as punching shear failure. Although local buckling of the CHS columns was not observed in any cases, the slender

column with 4 mm thickness, failed due to localised punching shear and highlighted the importance of the aforementioned design checks. In the configuration with 4mm thick CHS, yielding occurred on the CHS column surface prior to any yielding in the through I-beam web (Fig. 21a). Failure in such slender column connections was thus observed to be dominated by the local stress concentrations occurring in the CHS column surfaces near the I-beam flanges. In such cases, the through I-beam webs did not develop the failure stresses yet. On the other hand, for the configurations with a thicker CHS column (8, 10, 12.5 mm), the I-beam web yielded first (Fig. 21b) and failure occurred in the joint panel - combined failure of both the through I-beam web and the CHS column surface.

4.3 CHS column diameter (d_c)

The CHS column diameter was varied from 273 mm to 457 mm (Table 1). The diameters were chosen based on their availability in the steel construction industry. Force-displacement curves in Fig. 22 and 23 describes the effect of diameter variation for LC1 and LC2, respectively.

As the through I-beam was kept constant, the CHS column diameter did not have any significant effect on the vertical force-displacement curves for LC1. However, small differences were noticed (Fig. 22) due to the fact that V_{bb} is compared instead of $M_{pl,Rd,beam}$. As V_{bb} is derived from $M_{pl,Rd,beam}$ according to Eq. 19, it incorporates a small deviation due to d_c. Therefore, although small differences were noticed in the analytical values and force-displacement curves, the CHS column diameter failed to show any substantial effect in the joint configuration under LC1 from a behavioural perspective. In LC2, however, d_c played a noticeable role in influencing the joint strength as shown in Table 1 and Fig. 23. Successful

arguments were again observed in the FE models compared to the analytical calculations as the design approach was able to produce a more or less correct prediction regarding the failure mode and resistance for the LASTEICON configurations with different CHS diameters. von Mises equivalent stresses are not shown due to qualitative similarity.

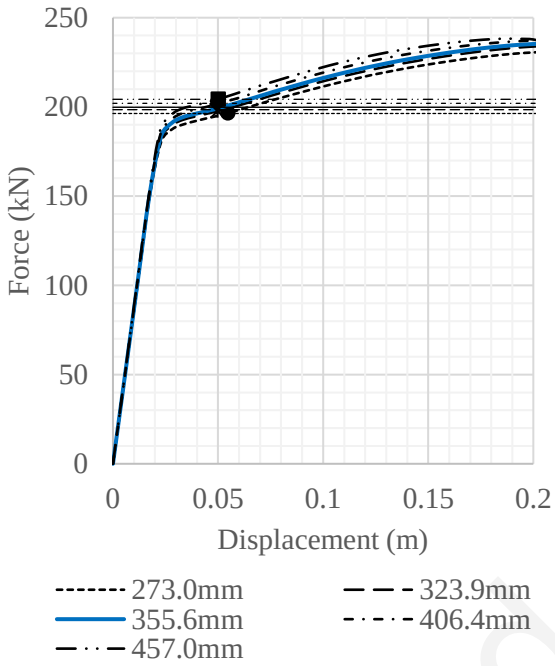

Fig. 22. *Vertical force-displacement curve comparisons for varying CHS column diameter under LC1*

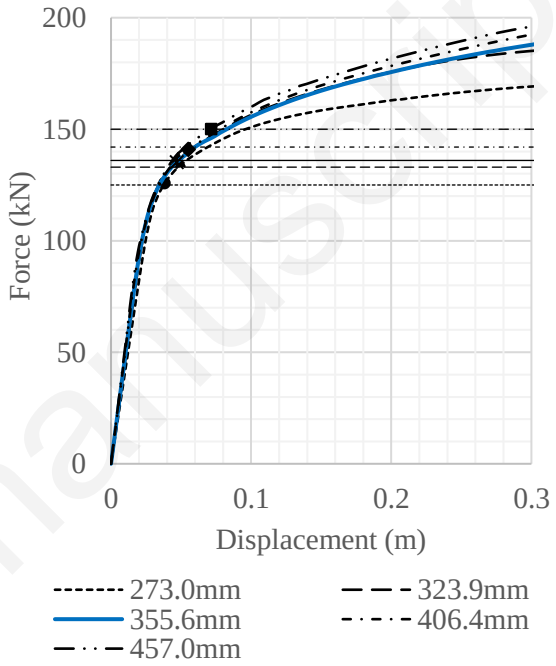

Fig. 23. *Vertical force-displacement curve comparisons for varying CHS column diameter under LC2*

4.4 Material properties for both CHS and through I-beam (f_{yb} and f_{yc})

Different steel grades were also chosen to identify the failure sequences in the joint panel. Primarily, nominal material properties were chosen for three different steel grades, S275 (f_y = 275 MPa), S355 (f_y = 355 MPa), and S450 (f_y = 440 MPa), to model all the members in the joint configuration ($f_{yb} = f_{yc}$) as shown in Table 1. f_y stands for the yield strength of a steel grade. In Fig. 24 and 25; "S275N", "S355N" and "S450N" refer to the numerical models with

635 the corresponding nominal material properties with strain hardening, adopted according to
636 Table 3.1 (EN 10025-2), EN 1993-1-1. “S355 Experiments” refers to the model with the
637 experimental material stress-strain properties i.e. a combination of yield strengths for the
638 beams and the CHS column (f_{yb} =355 MPa and f_{yc} = 377 MPa). Furthermore, “S355N-S450N
639 (B-T)” defines a material combination where the beam was modelled with S355N and the
640 CHS column is constructed with S450N, whereas, “S450N-S355N (B-T)” denotes the opposite
641 combination.

642 As shown in Fig. 24, the force-displacement curves for “S355N” and “S450N”
643 overlapped with “S355N-S450N (B-T)” and “S450N-S355N (B-T)” respectively, for LC1.
644 Similar results were noticed from the V_{bb} values calculated in Table 1. This validated the
645 aforementioned conclusion that the failure under LC1 is solely dominated by flange buckling
646 of the through I-beam. A significant difference was noticed between the force-displacement
647 curves of “S355N” and “S355 Experiments” due to the difference in the ultimate stress and
648 strain of the corresponding material curves. However, no exact overlap was noticed in the
649 force-displacement curves under LC2 (Fig. 25). This justified the previous interpretation that
650 both the through I-beam and the CHS contributes to the ultimate joint resistance.
651 Additionally, the analytical value and the force-displacement curve for “S355N-S450N (B-T)”
652 were closer to those for “S450N” compared to “S355N” and similarly, “S450N-S355N (B-T)”
653 was closer to “S355N” than “S450N”. This observation possibly highlights a slightly larger
654 contribution offered by the CHS compared to the through I-beam under LC2.

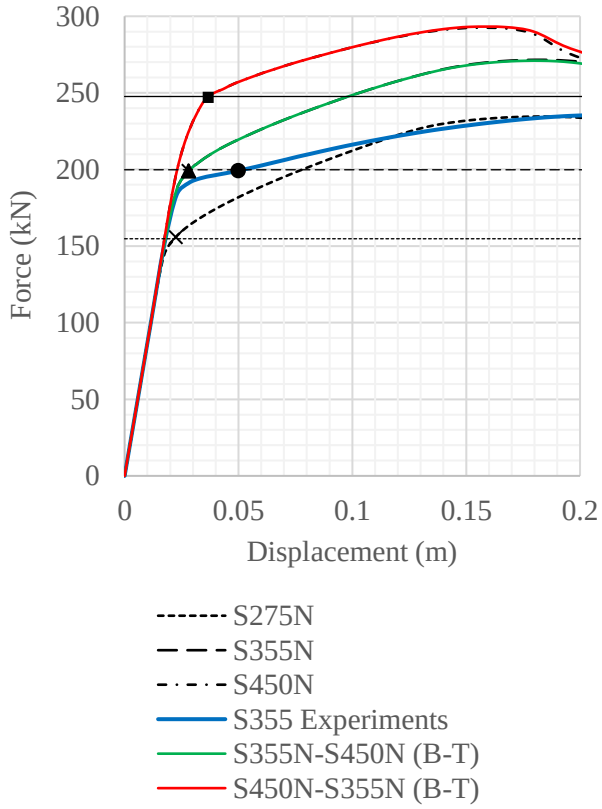

Fig. 24. *Vertical force-displacement curve comparisons for varying steel grades under LC1*

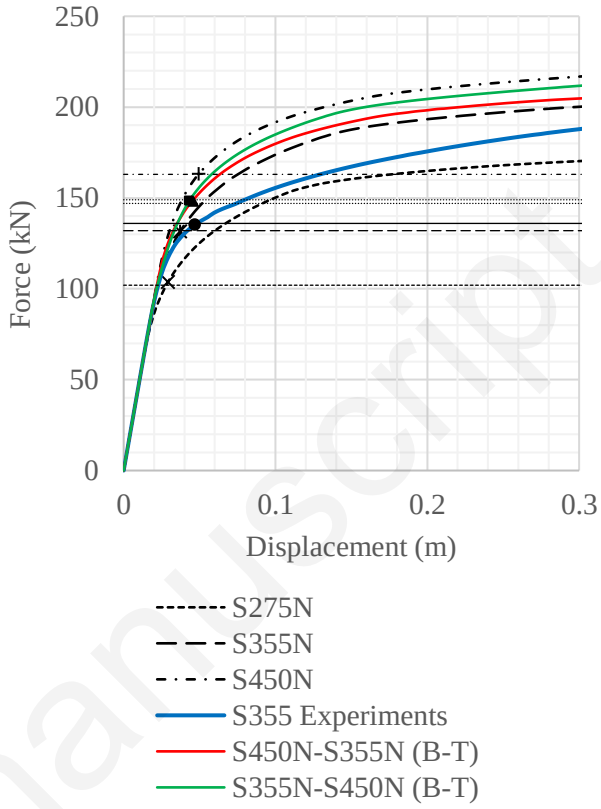

Fig. 25. *Vertical force-displacement curve comparisons for varying steel grades under LC2*

4.5 Moment-to-Shear (M/V) Ratio

In order to check the consistency of the proposed design approach, the joint configurations were investigated for different M/V ratios. The M/V ratio was varied by varying the total length of the beam, L_b, thus changing the lever arm between the CHS column wall face and the extremity at which the vertical load is applied. However, the through I-beam length was kept constant as shown in Fig. 13. Decreasing L_b decreased the M/V ratio and therefore, for a certain vertical load (shear force) the joint configuration experienced a smaller moment compared to the reference configuration. The contrary happened for an increased L_b. The

force-displacement curves are compared with relevant analytical calculations in Fig. 26 and 27 for LC1 and LC2, respectively. Good agreements were achieved between the analytical and numerical results thus confirming the consistency of the proposed design approach.

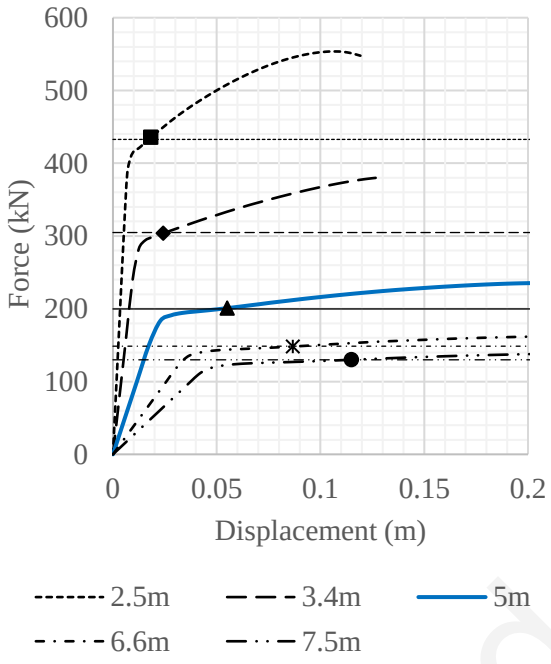

Fig. 26. *Vertical force-displacement curve comparisons for varying beam length under LC1*

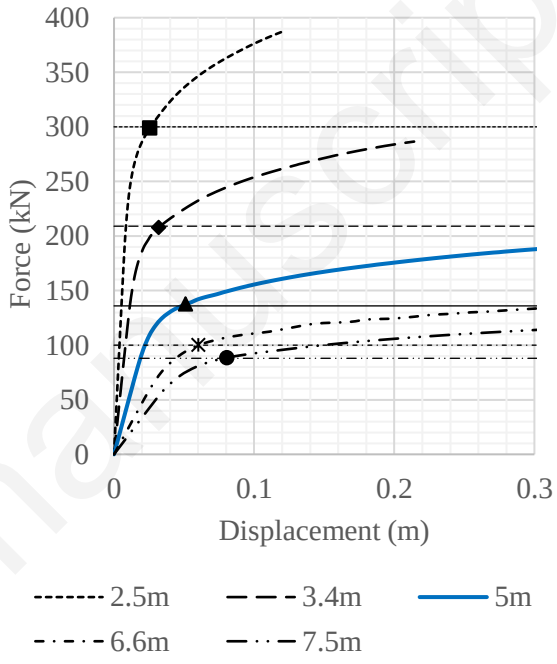

Fig. 27. *Vertical force-displacement curve comparisons for varying beam length under LC2*

4.6 Comparison with Conventional I-beam-to-CHS joint configurations

As discussed in Section 1 and 3, the conventional joint configurations involving an I-beam and a CHS column are not completely capable of utilizing the advantages provided by the hollow sections. Therefore, a short comparison study was done in order to see the potential advantages of the proposed LASTEICON "passing-through" I-beam-to-CHS column connection. As the CHS column governs the failure modes of such conventional connections,

the CHS column thickness alone was varied to check the minimum thickness required for these conventional connections to reach the strength of the reference LASTEICON configuration, which was kept constant throughout the parametric study. This reference configuration constituted of an IPE400 section passing through a CHS column with 355.6 mm diameter (d_c) and 10 mm thickness (t_c) with a total beam length (L_b) of 5000 mm. However, the conventional joints were modelled by simply removing the "passing-through" part of the inserted IPE beam as well as the slots in the CHS columns. The force displacement curves are compared in Fig. 28 and 29 for LC1 and LC2, respectively.

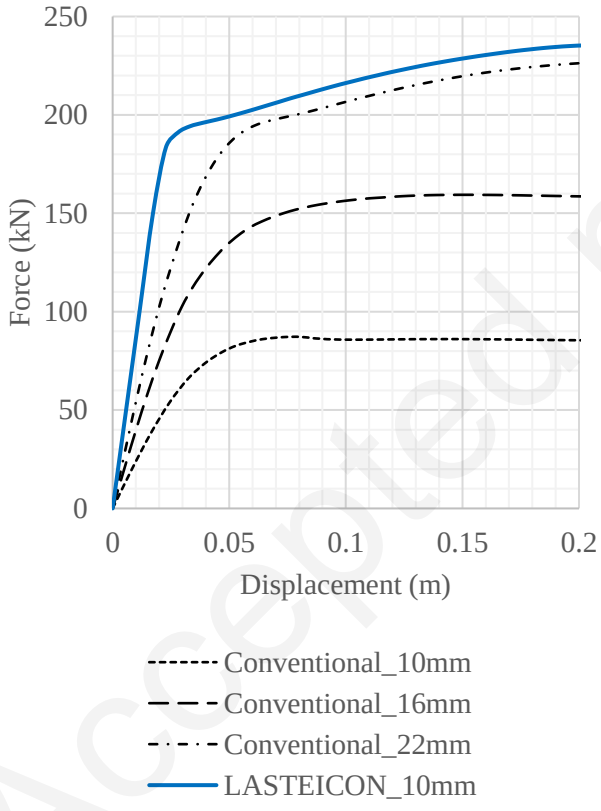

Fig. 28. *Vertical force-displacement curve comparisons between LASTEICON and conventional plate-to-CHS connection under LC1*

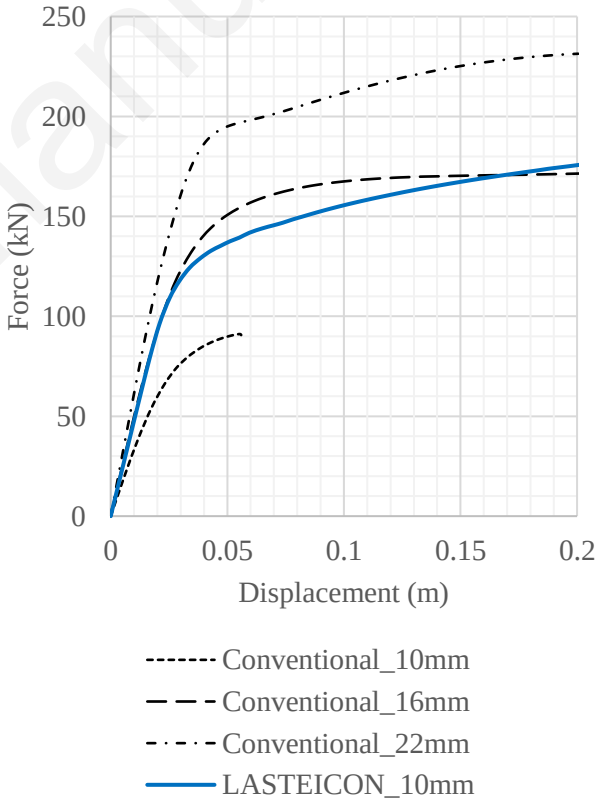

Fig. 29. *Vertical force-displacement curve comparisons between LASTEICON and conventional plate-to-CHS connection under LC2*

As the through I-beam solely dominates the failure under LC1, significant advantages were observed in the force-displacement curve comparisons as shown in Fig. 28. A conventional configuration with 22mm thick CHS column only proved to be sufficient to provide as much resistance as the LASTEICON configuration with a 10 mm thick CHS column under LC1. A significant decrease in the stiffness was also observed due to the removal of the "passing-through" part. Under LC2, a 16 mm thick column in the conventional configuration sufficed to be enough resisting as the LASTEICON joint with 10mm thickness as shown in Fig. 29. This proves a significant contribution of the "passing-through" I-beam towards strengthening the joint panel.

5. DISCUSSIONS AND REMARKS

A parametric study was done based on a series of nonlinear static analyses in accordance with the EN 1993-1-1 and EN 1993-1-8 prescriptions in order to construct a conservative design method for the proposed "passing-through" I-beam-to-CHS connection. The design hypothesis was developed based on a successful identification of the force-transfer mechanism and was further validated through numerical simulations and experimental results. Based on encouraging results, this newly proposed LASTEICON connection as well as its design procedure can be concluded as an efficient upgrade to the conventional I-beam-to-CHS column connections with direct welds. The following points highlights the noteworthy findings of this research study.

- In the monotonic gravitational loading LC1, both vertical forces were applied in the same direction, thus generating equal and opposite moments on either side of the CHS

column surface. These moments nullified each other, which led to a rigid body like behaviour of the actual "passing-through" joint panel. As a result, the ultimate joint strength (and failure) was solely governed by the plastic flexural resistance of the through I-beam just outside the CHS.

- In the opposite bending loading LC2, both the through I-beam as well as the CHS column contributed significantly towards developing the ultimate joint strength. For properly designed joints (i.e. safe from the three checks mentioned in the design procedure), failure occurred simultaneously in the through I-beam web (due to transverse shear) and the CHS column surface (due to transverse tensile/compressive forces), thus validating the anticipated force-transfer mechanism and the corresponding design procedure.
- Under LC2, while increasing the through I-beam section offered greater strength and stiffness, reducing it showed substantial vulnerability towards flexural failure of the through beam prior to full activation of the joint panel strength, justifying the first check suggested in the design procedure.
- To validate the second and third check, regarding the local buckling and punching shear failure respectively, few class 3 and 4 type CHS columns were deliberately chosen in the proposed configuration to examine the prediction accuracy of the design calculations. According to the design calculations, the 4 mm thick CHS column connection failed due to localized punching shear on the CHS column surface, prior to activation of the complete joint strength. The 6 mm thick CHS connection marginally avoided such a punching shear failure. The failure mode for Class 1 and 2 CHS columns

was observed to be the joint panel failure. These observations justified the requirement of Design check 3. However, to avoid such irregular failures, it is better to avoid the class 3 and 4 type CHS while constructing such "passing-through" connections. Similar encouraging agreements were found between the analytical and numerical models for CHS diameter variation.

- In real life structures, as the CHS column would be axially loaded rather than being an unloaded part of the joint configuration, significant compressive forces might make it vulnerable towards local buckling failure. Even though only one local buckling failure was observed in the present range of investigations, design check 2 is therefore recommended to avoid such a failure.
- Parametric studies with varying material properties and different material combinations made it evident that failure under LC1 was solely dominated by the through I-beam and failure under LC2 depended on both the through I-beam web as well as the CHS column for the proposed configuration safe from all the checks. Furthermore, these studies also hinted a slightly larger contribution from the CHS column compared to the through I-beam in developing the ultimate joint strength under LC2. Encouraging results supported the consistency of the suggested design approach for varying M/V (Moment-to-shear) ratios.
- Furthermore, a comparative study between the conventional and the LASTEICON configurations showed the advantages provided by the passing-through elements in terms of strength and stiffness of the whole joint. In a conventional configuration under LC1, the CHS column had to be made at least 2.2 times thicker to acquire an

776 equal resistance as a LASTEICON connection with similar geometric/sectional
777 properties. However, under LC2, a 1.6 times thicker CHS column proved to be
778 adequate.

779 • As mentioned in Section 1, the laser cutting technique surpasses the other cutting
780 methods. Much lower amounts of slag are released during the fabrication of the joint
781 assembly due to a simpler and reduced welding, thanks to the higher precision offered
782 by the laser [34-36]. Additionally, the heat affected zones (HAZ) of laser cutting is
783 much smaller, when compared to other methods [36]. Nevertheless, to refine the
784 knowledge regarding the joint capacity, additional attention should be paid to the HAZ
785 due to LCT and on the welding operation between the passing through elements and
786 the slotted CHS column. Although the LCT reduces the importance of the HAZ
787 significantly compared to the classical cutting procedures [24], additional
788 experiments are still required to better quantify the LCT/welding interaction. The
789 feasibility of cutting inclined angles was reported in a first study [24] for joints with
790 thin CHS columns (≤ 10mm), discussing the possibility of full penetration welds in the
791 proposed connection, which resulted in a shorter fabrication time as well as an
792 increased ductility compared to the fillet welds. Additional studies are currently
793 ongoing to obtain full penetration welds above 10 mm thickness by controlling the
794 chamfer angle and the gap size. The results achieved so far and presented in [32]
795 however show that, in this range of thicknesses, the connections with fillet welds
796 perform better in terms of global strength than connections with full penetration
797 welds.

798

6. CONCLUSION

A new configuration for an open-to-hollow section joint with a “passing though” concept is proposed in this paper through the “LASTEICON” project funded by the European Commission. This type of an I-beam-to-CHS column joint is recommended for using in structures with predominant gravitational as well as opposite bending loading. The unique component of this joint is a through I-beam supporting the primary beams. Knowing the applied loads, the geometries and the materials, a design procedure is further proposed to calculate the resistance offered by such connections. The procedure is verified through a detailed numerical parametric analysis which is validated by an experimental campaign. Emphasis is put onto the generation of global models that are suitable to predict the ultimate resistance of the proposed joint configurations. These models can be used to assess the load transfer, stress concentrations and possible failure modes correctly with respect to the experimental investigations. Strong agreements are obtained between the design analytical calculations and the experimentally calibrated numerical simulations. Additional experimental results are however required to extend the validated range of application of the design procedure and are planned for the near future considering different loading conditions with axial compression/tension, different welding types and real-life uncertainties.

ACKNOWLEDGEMENTS

This research study was possible thanks to the research fund provided by the European Commission with the contract LASTEICON EU-RFCS GA-709807 (www.LASTEICON.eu). The project consortium includes Fincon Consulting Italia srl (coordinator), RWTH Aachen, University of Pisa, Hasselt University, Instituto Superior Tecnico of Lisbon and INSA Rennes, ADIGESYS, OCAM and VALLOUREC. The cooperation of all of them is hereby gratefully acknowledged.

REFERENCES

[1] J. Wardenier, J.A. Packer, X.L. Zhao, and G.J. Van der Vegte, Hollow Sections in Structural Applications, CIDECT, Geneva, Switzerland, 2010.

[2] J. Wardenier, Y. Kurobane, J.A. Packer, G.J. van der Vegte and X.L. Zhao, Design guide for circular hollow section (CHS) joints under predominantly static loading, CIDECT Design Guide 1, Geneva, Switzerland, 2008.

[3] J. Rondal, K.G. Würker, D. Dutta, J. Wardenier, and N. Yeomans, Structural stability of hollow sections, CIDECT Design Guide 2, Verlag TUV Rheinland GmbH, Köln, Germany, 1992.

[4] D. Dutta, J. Wardenier, N. Yeomans, K. Sakae, O. Bucak, J.A. Packer, Design guide for fabrication, assembly and erection of hollow section structures, CIDECT Design Guide 7, ISBN 3-8249-0443-8, TÜV-Verlag GmbH, Köln, Germany, 1998.

[5] Y. Kurobane, J. A. Packer, J. Wardenier, N. Yeomans, Design Guide for Structural Hollow Section Column Connections, CIDECT Design Guide 9, ISBN 3-8249-0802-6, TÜV-Verlag GmbH, Köln, Germany, 2004.

[6] J.P. Jaspart, K. Weynand, Design of hollow section joints using the component method, Proc. 15th Int. Symp. Tubul. Struct (ISTS) (2015) 405–410, Rio Janeiro, Brazil.

[7] K. Weynand, J.P. Jaspart, Application of the component method to joints between hollow and open sections, CIDECT project 5BM, 2015.

851 [8] J.P. Jaspart, C. Pietrapertosa, K. Weynand, E. Busse, R. Klinkhammer and J.P. Grimault,
852 Development of a full consistent design approach for bolted and welded joints in
853 building frames and trusses between steel members made of hollow and/or open
854 sections - application of the component method volume 1 - practical guidelines,
855 CIDECT Report : 5BP-4/05, August 2005.

856 [9] J. Wardenier, Semi-rigid connections between I-beams and tubular columns, Final
857 Report, ECSC-EC-EAEC, Brussels. Luxembourg, 1995.

858 [10] Y.M. Alostaz, S.P. Schneider, Connections to concrete-filled steel tubes, A Report on
859 Research Sponsored by the NATIONAL SCIENCE FOUNDATION NSF CMS 93-00682.

860 [11] W. Wang, Y. Chen, and W. Li, R. Leon, Bidirectional seismic performance of steel beam
861 to circular tubular column connections with outer diaphragm, Earthquake
862 Engineering and Structural Dynamics, 40 (2010) 1063–1081.

863 [12] A. B. Sabbagh, T.M. Chan, and J.T. Mottram, Detailing of I-beam-to-CHS column joints
864 with external diaphragm plates for seismic actions, Journal of Constructional Steel
865 research 88 (2013) 21–33.

866 [13] T. Fukumoto, K. Morita, Elastoplastic behavior of panel zone in steel beam-to-concrete
867 filled steel tube column moment connections, ASCE Journal of Structural Engineering
868 131 (2005), 1841–1853.

869 [14] I. Nishiyama, T. Fujimoto, T. Fukumoto, and K. Yoshioka, Inelastic force-deformation
870 response of joint shear panels in beam-column moment connections to concrete-filled
871 tubes, ASCE Journal of Structural Engineering 130 (2004) 244–252.

872 [15] S. Morino, K. Tsuda, Design and construction of concrete-filled steel tube column
873 system in Japan, Earthquake Engineering and Engineering Seismology, 4 (2002) 51–
874 73.

875 [16] T. Fujimoto, E. Inai, M. Kai, K. Mori, O. Mori, and I. Nishiyama, Behavior of beam-to-
876 column connection of CFT column system, 12th World Conference on Earthquake
877 Engineering (2000) 1–8.

878 [17] Tata Steel, Steel Construction Cost. The British Constructional Steelwork Association,
879 2013.

880 [18] S.R. Mirghaderi, S. Torabian, and F. Keshavarzi, I-beam to box-column connection by
881 a vertical plate passing through the column, Engineering Structures 32 (2010) 2034–
882 2048.

883 doi:10.1016/j.engstruct.2010.03.002.

884 [19] A.P. Voth, J.A. Packer, Branch Plate-to-Circular Hollow Structural Section Connections.
885 I: Experimental Investigation and Finite-element Modeling, ASCE Journal of Structural
886 Engineering 138 (8) (2012) 1007–1018. doi: 10.1061/(ASCE)ST.1943-
887 541X.0000545.

888 [20] A.P. Voth, Branch Plate-to-Circular Hollow Structural Section Connections, Doctoral
889 Thesis, 2010.

890 [21] Y.M. Alostaz, S.P. Schneider, Analytical behavior of connections to concrete-filled steel
891 tubes, Journal of Constructional Steel research 40 (1996) 95–127.

892 [22] A. Kanyilmaz, The problematic nature of steel hollow section joint fabrication, and a
893 remedy using laser cutting technology: A review of research, applications,
894 opportunities, Engineering Structures, 183 (2019) 1027-1048.

895 [23] C.A. Castiglioni, A. Kanyilmaz, W. Salvatore, F. Morelli, A. Piscini, M. Hjiaj, M. Couchaux,
896 L. Calado, J.M. Proença, B. Hoffmeister, J. Korndörfer, H. Bigelow, H. Degee, R. Das, S.
897 Raso, A. Valli, M. Brugnolli, A. Galazzi, R. Hojda, EU-RFCS Project LASTEICON (Laser
898 Technology for Innovative Joints in Steel Construction), (2016). www.LASTEICON.eu.

899 [24] A. Kanyilmaz, and C.A. Castiglioni, Fabrication of laser cut I-beam-to-CHS-column steel
900 joints with minimized welding, Journal of Constructional Steel Research 146 (2018)
901 16–32.

902 [25] A. Elremaily and A. Azizinamini, Design provisions for connections between steel
903 beams and concrete filled tube columns, Journal of Constructional Steel Research,
904 57(9) (2001) 971–995.

905 [26] European Committee for Standardization, Eurocode 3: Design of Steel Structures -
906 Part 1–1: General Rules and Rules for Buildings. EN 1993-1-1, 2005.

907 [27] European Committee for Standardization, Eurocode 3: Design of steel structures -
908 Part 1-8: Design of joints. EN 1993-1-8, 2005.

909 [28] Final Document of prEN 1993-1-8. European Committee for Standardization,
910 Eurocode 3: Design of steel structures - Part 1-8: Design of joints, EN 1993-1-8, 2018.

911 [29] J. Wardenier, Hollow Sections in Structural Applications, Delft University of
912 Technology, Netherlands, December 2001.

913 [30] DIANA User's Manual, DIANA Release 10.2, May, 2018.

914 [31] DIANA User's Manual, Element Library. User's Manual Release 9.5, February, 2014.

[32] M. Couchaux, V. Vyhlas and M. Hjiaj, RFCS Project LASTEICON Test Report: Tests on Joints C3 and C4, INSA, Rennes, March 2019.

[33] B. Hoffmeister, M. Wieschollek, RFCS Project MECADO (RFSR-CT-2013-00022), Deliverable 2.2 - Cyclic behaviour of class 3 or 4 steel and composite sections - Numerical simulations, Aachen, Germany, 2017.

[34] R. Aloke, V. Girish, R.F. Scrutton, P.A. Molian, A model for prediction of dimensional tolerances of laser cut holes in mild steel thin plates, Int. J. Mach. Tools Manuf. 37 (1997) 1069–1078, https://doi.org/10.1016/S0890-6955(96)00090-9.

[35] Davilla Group n.d. http://www.davilla.it/en/taglio-laser-tubo.aspx.

[36] M. Harničárová, J. Zajac, A. Stoić, Comparison of different material cutting technologies in terms of their impact on the cutting quality of structural steel, Tech Gaz 17 (2010) 371–376.